ANALYTICAL MODELING OF CONDUCTIVITY CHEMOGRAPHS OF BYRDS MILL SPRING

By

JOHN GARRETT RICHINS

Bachelor of Science in Geology

Oklahoma State University

Stillwater, OK

2014

Submitted to the Faculty of the
Graduate College of the
Oklahoma State University
in partial fulfillment of
the requirements for
the Degree of
MASTER OF SCIENCE
December, 2020

ANALYTICAL MODELING OF CONDUCTIVITY

CHEMOGRAPHS OF BYRDS MILL SPRING

Thesis Approved:

Dr. Todd Halihan

Thesis Advisor

Dr. Ali Mirchi

Dr. James O. Puckette

ACKNOWLEDGEMENTS

I would like to thank Dr. Halihan for working with me over the last ten years, both as an undergraduate and a graduate student. I became interested in groundwater after taking his Hydrogeology course as an undergraduate. His class made me take an interest in learning and diving deeper into a subject that interested me, rather than just getting through the surface level of material required for the course. His time and patience has allowed me to develop into the hydrogeologist that I am today. He has taught me how to critically approach and address problems and think like a scientist.

I would like to thank the OSU field team, consisting of Courtney Hall and Jeff Payne, for their integral part in collecting crucial field data. Without their work, this thesis would not be possible. A great deal of gratitude also goes out to Randel Ross, of the EPA, who was always available to grant us access to the site and bounce questions off of. Additionally, I am grateful to the many others that have helped throughout this process.

Last, but certainly not least, I would also like to thank my wife, Alison, who has been with me at every obstacle helping me get through it. I am grateful for her constant encouragement, even when her front-row-seat meant putting up with any thesis frustrations I brought home. Without her, I would not have been able to finish and I want to thank her for standing by my side through it all.

Name: JOHN RICHINS

Date of Degree: DECEMBER, 2020

Title of Study: ANALYTICAL MODELING OF CONDUCTIVITY CHEMOGRAPHS OF BYRDS MILL SPRING

Major Field: GEOLOGY

Abstract: Rhythmic springs occur when a groundwater flowpath that supplies a spring's discharge form a hydraulic siphon. The hydraulic siphon brings the spring varying fluxes of water that cycle over time. If these flows are only one flowpath in the total spring system, the influx of water from the siphon may have strong effects on water quality, but be difficult to detect in hydrograph data during spring storm response. Oscillations in electrical conductivity data were observed at Byrds Mill Spring, Pontotoc County, Oklahoma (USA). Byrds Mill Spring is the largest spring in Oklahoma by volume, and oscillations in electrical conductivity were observed during a set of extreme precipitation events in May 2015. A data logger placed at the spring's outflow recorded the electrical conductivity of the spring's oscillating between 520 µS/cm and 10 µS/cm multiple times while discharge remained steady.

A numerical tank model was developed to simulate the electrical conductivity chemograph of Byrds Mill Spring to test hypotheses about the geometry of the siphoning system. The model simplified the karst system as a tank connected to a siphoning drain and a tank connected to a non-siphoning drain joined together by mixing at a T-junction. Using this approach, the model was able to reproduce key features of the Byrds Mill Springs chemograph. The model results provide controls on where the siphon may be located and the dimensions of the siphon system.

TABLE OF CONTENTS

Chapter Page

LIST OF TABLES

Table Page

LIST OF FIGURES

Figure Page

LIST OF EQUATIONS

CHAPTER I

INTRODUCTION

Karst aquifers provide a source of drinking water to people around the world. Studies have shown that 10% to 25% of humanity relies on karst aquifers for their primary water source (Stevanović, 2019). Stable baseflow of karst aquifers provide a consistently reliable volume of water supply, but the stability of this source can be affected by surface water rapidly moving through aquifers through karst conduits and fractures (Atkinson, 1977).

Karst aquifers are formed when water dissolves soluble rock to enlarge flowpaths (fractures and conduits) (White, 1988; Bonacci and Bojanić, 1991). These enlarged flowpaths provide conveyance for quickflow, where water moves from the surface or other parts of the aquifer at a rapid rate (Atkinson, 1977). Quickflow can greatly change the discharge rate and/or chemical composition of a spring (Atkinson, 1977; Halihan and Wicks, 1998).

Karst flowpaths sometimes form in a way so that hydraulic siphon structures are created in the subsurface (Bonacci and Bojanić, 1991). When a spring's discharge is controlled by these siphons, it causes the phenomena known as rhythmic springs (Bonacci and Bojanić, 1991). The discharge from rhythmic springs creates an oscillating pattern of peaks and troughs when observed on a hydrograph. Peaks indicate periods of high flows where the siphon is operational and troughs indicate periods of low flow where the siphon is not operational (Bonacci and Bojanić, 1991).

Birds Mill Spring (BMS) is a stable karst spring that provides the City of Ada, Oklahoma with its

primary drinking water supply (Ada). BMS's fluid electrical conductivity (EC) is usually a consistent level of approximately 520 µS/cm; in March of 2015, EC data collected from BMS showed that the spring chemistry became unstable during a set of large rainfall events. The EC of BMS oscillated between the normal baseflow of 520 µS/cm and dropped to 10 µS/cm of pure rainwater (Zdeb, 2018).

BMS discharges from a dolomitic karst aquifer known as the Eastern Arbuckle-Simpson aquifer. Due to the inaccessibility of the karst system's secondary porosity, little is known about the geometries of passages and fractures that transport water within the aquifer to BMS. Testing the mechanics of fluid EC oscillation may provide insight into the geometries of the passages and fractures. If pure rainwater is entering BMS, a direct conveyance from the surface to BMS exists with the potential to negatively impact the water supply quality. Knowing the geometry and properties of this flowpath allows for land management measures to be put into place to protect BMS from surface impacts.

Investigating the mechanics of how the conveyance at BMS operates to provide an oscillation of freshwater input gives us a deeper insight into how surface water interacts with groundwater in karst systems. The mixing of these flowpaths is also critical to understanding what percentage of a flow system could be overcome by a rapid pathway relative to baseflow conditions at a spring. This thesis will test the potential cause of these oscillations by modeling potential physical mechanisms for a structurally-complex karst system, which could produce such effects.

A numerical siphon model was created to test the functioning of a hypothesized siphon connected to BMS, and to determine the approximate location and dimensions of the siphon's hydraulic features. An analytical reservoir and siphon model were created to model EC chemograph patterns that were compared to the field data collected from BMS. If the model outputs are similar to the

field data, the presence of a siphon and associated mixing processes will be supported by the model and provide insight for additional field investigations.

CHAPTER II

REVIEW OF LITERATURE

Models of karst aquifers have often diverged from the porous media models used in other aquifers. The structure of permeability in these systems means other models are needed to evaluate the controls on these aquifers, such as various reservoir and pipe models, along with models that simulate the effects of hydraulic siphons and mixing. This literature review will evaluate numerical models and analytical models of karst. Additionally, the literature of modeling siphons and groundwater mixing processes will be discussed.

Numerical Models in Karst

Numerical models have been used to test processes and evaluate various karst flow patterns. These models simplify the complexity of the natural systems by breaking down the fluid process into equations representative of the active physical and chemical processes. One type of numerical model is the analytical tank model. These tank models have been used by several different researchers to evaluate problems in karst hydrology (Campana and Mahin, 1985; Bonacci and Bojanić, 1991; Halihan and Wicks, 1998). As this work utilizes analytical modeling techniques, the review will evaluate previous work using this type of approach.

Analytical Models

Several researchers have simplified karst systems by modeling large cave rooms and constrictive cave passages as tanks and pipes. Analytical tank models simplify the geometry of karst systems

by breaking the system into manageable pieces. Large cave reservoirs are thought of as tanks and small/constricted cave passages are thought of as pipes (Halihan and Wicks, 1998).

Campana and Mahin (1985) used a discrete-state compartment model to determine groundwater mean ages, recharge, effective porosities, and storage in the Edwards aquifer (Campana and Mahin, 1985). Bonacci and Bojanić (1991) created a model to reproduce the discharge of rhythmic springs. The model was set up so that a cave reservoir (tank) drained through a siphoning pipe, creating the desired effect in the discharge pattern (Bonacci and Bojanić, 1991).

This analytic tank model approach was also used to describe storm response in a constricted flow cave with a reservoir representing the aquifer and conduit system, with a pipe representing a flow constriction just upgradient from the spring (Halihan et al., 1998). Using a series of equations, the modelers were able to demonstrate how constrictions in the cave passage of Devil's Icebox cave governed flow through the system. Turbulent pipe flow equations were used to represent how water flowed through a constricted cave passage. The model was able to generally replicate field-collected storm response data using this approach.

Rhythmic Spring Mechanism

Numerical models have been used to explain how rhythmic springs (ebb & flow springs or intermittent springs) operate. Using these models, researchers have been able to quantify the physical properties that control these springs (Bonacci and Bojanić, 1991). The models typically employ a larger cave reservoir connected to a smaller siphon cave that runs to a spring. When water levels in the cave reservoir rise above the top of the siphon, the siphon becomes primed and begins to drain the reservoir. Once the reservoir is drained, air enters the siphon cave, and flow stops (Bonacci and Bojanić, 1991).

The siphon's starting and stopping of the flow create an oscillating pattern when recorded on a spring hydrograph. Two distinct hydrograph patterns for rhythmic springs (*Figure 1*) were

described by Bonacci and Bojanić (1991): a) a continuous basic flow with rhythmic discharge added and b) no continuous basic flow, only rhythmic discharge added.

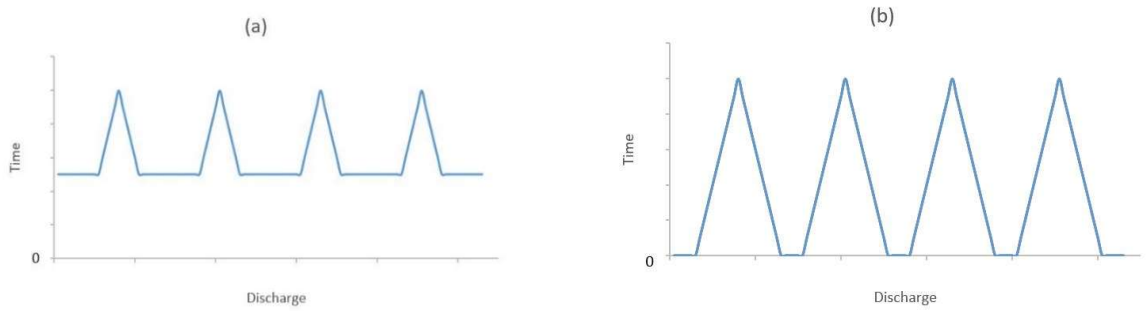

Figure 1: Hydrograph patterns of continuous rhythmic springs. (a) Baseflow with rhythmic discharge added; (b) No continuous base flow, only rhythmic discharge added.

It is well defined on how siphons affect a spring's discharge, but no previously published research was found on how siphons can affect the EC of a spring. This thesis will attempt to determine how a siphon can affect the EC of a spring by combining karst flow and groundwater mixing models.

Karst Groundwater Mixing

Previous research on karst groundwater mixing has been performed to determine how different fluids interact with each other in conduits and fractures (Park and Lee, 1999; Johnson et al., 2006). Mixing in large tanks, or in this case large caves, has been well documented (García et al., 1993; Holzner, 2008; Agarwal, 2019). The concentration of waters with two different chemistries has been described using a differential equation (Holzner, 2008; Agarwal, 2019). These interactions can be expressed mathematically so the function can be modeled. The mixing process for this research is important in two locations for the physical system, one as the recharge enters the system and the second where siphon water mixes with the regional flow of the aquifer.

Water in karst aquifers primarily travels through secondary porosity pathways. These pathways occasionally intersect, forming junctions where water mixes. This mixing can be simulated as streamline routing or complete mixing (Park and Lee, 1999; Johnson et al., 2006). When complete

mixing occurs, two fluids meet at an intersection and discharge as a homogenous mixture through the outlet (Park and Lee, 1999; Johnson et al., 2006). Streamline routing occurs when two fluids intersect and are routed into outlet fractures without much physical mixing occurring. Streamline routing can be continuous or discontinuous (Park and Lee, 1999; Johnson et al., 2006). Continuous streamline routing occurs when the fluids entering the intersection exit through the same outlet. The concentration of the outlet is dependent on the ratios of the inlet flow amounts (*Figure 2*a). Discontinuous streamline routing occurs when two fluids meet at an intersection and are routed in adjacent outlets with very little mixing occurring (*Figure 2*b) (Park and Lee, 1999; Johnson et al., 2006).

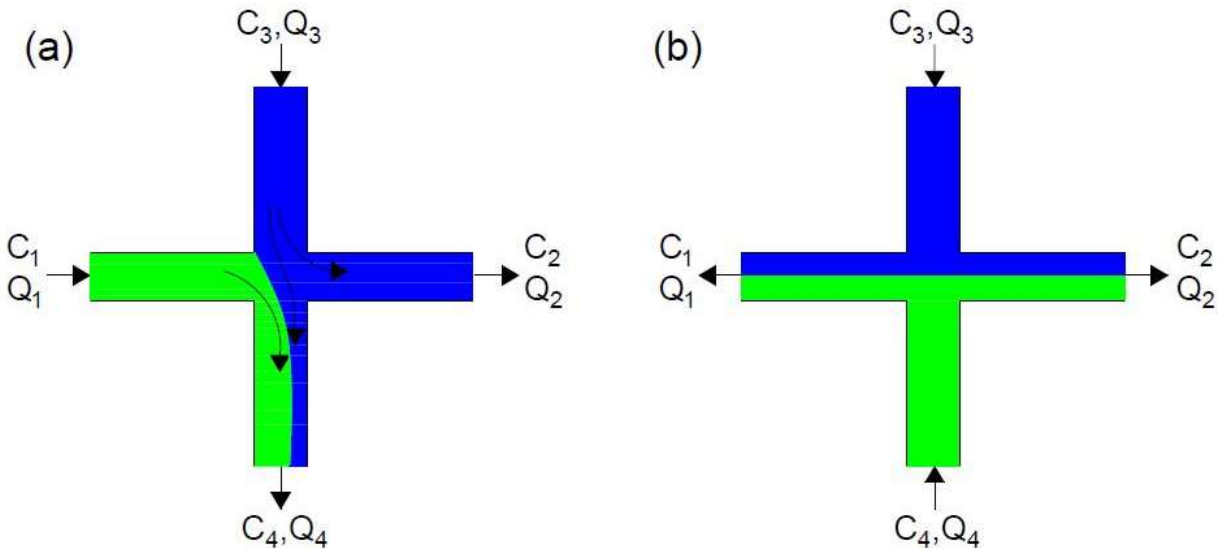

Figure 2: Two types of streamline routing affecting discharge, Q, and concentration, C, of the mixing system. (a) Continuous streamline routing occurs when the fluids entering the intersection exit through the same outlet. (b) Discontinuous streamline routing occurs when two fluids meet at an intersection and are routed in adjacent outlets with very little mixing occurring (Park and Lee, 1999; Johnson et al., 2006).

Researchers have expressed the mathematics of how fluid flows through the junction (Park and Lee, 1999; Johnson et al., 2006). Continuous flow is governed by two equations. The discharge of continuous flow mixing may or may not include both fluids. The first equation describes how two fluids of different concentrations mix when the inflow is less than the outflow (Equation (1)). The

equation for continuous flow where the inlet flow of one fluid (Q_1) is less than the outlet flow of the discharge location of that fluid (Q_4) is:

$$C_4 = C_1\left(\frac{Q_1}{Q_4}\right) + C_3\left(1 - \frac{Q_1}{Q_4}\right) \quad (1)$$

$$C_2 = C_3 \quad (2)$$

where Q is the flow rate, C is the fluid concentration, and subscript numbers correspond to inlet and outlet flows and concentration (*Figure 2*a) *(Park and Lee, 1999; Johnson et al., 2006)*.

The second continuous flow equation describes how two fluids of different concentrations mix when the inflow is more than the outflow (*Figure 2*a). In this case the equation is:

$$C_2 = C_3\left(\frac{Q_3}{Q_2}\right) + C_1\left(1 - \frac{Q_3}{Q_2}\right) \quad (3)$$

$$C_4 = C_1 \quad (4)$$

where Q is the flow rate, C is the fluid concentration, and the subscript numbers correspond with inlet and outlet quantities (*Figure 2*a) *(Park and Lee, 1999; Johnson et al., 2006)*.

Discontinuous flow can be simulated using a similar equation where the concentration of the discharge is dependent on the ratios of the two inflow rates. If both fluids are entering the junction, discontinuous flow's discharge will include a percentage of both fluids resulting in a calculated concentration of:

$$C_1 = C_2 = \frac{C_3Q_1 + C_4Q_4}{Q_3 + Q_4} \quad (5)$$

where Q is the flow rate, C is the fluid concentration, and the subscript numbers correspond with inlet and outlet amounts (*Figure 2*b) *(Park and Lee, 1999; Johnson et al., 2006)*.

Mixing of karst waters can also occur in large caverns. Basic mixing of multiple fluid chemistries in large voids (tanks) has been well tested. The classic differential equation problem of saline water being piped into a tank of freshwater tells how the water chemistry changes over time (Equation **(6)**) (Holzner, 2008; Agarwal, 2019). This equation shows the change in the tank's fluid concentration relative to a change in time by taking the difference of the entering and exiting fluid's flow rate and concentration (Holzner, 2008; Agarwal, 2019). This method provides a simple solution for analyzing the rate at which water of different chemistries mix in a large void. The equation is:

$$\frac{dC}{dt} = (\text{Rate in}) - (\text{Rate out}) \quad \textbf{(6)}$$

where dC is the change in concentration, dt is the change in time, *Rate in* is the rate at which a fluid of a certain concentration the tank enters the tank, and *Rate out* is the rate at which a fluid of a certain concentration exits the tank.

CHAPTER III

SITE DESCRIPTION

Byrds Mill Spring is located in the Eastern Arbuckle-Simpson aquifer and is the largest spring in the state of Oklahoma. It is the primary source of water for the City of Ada, Oklahoma. The spring location will be described by first discussing the geologic setting followed by the hydrologic setting.

Geologic Setting

The Arbuckle-Simpson aquifer is a major aquifer in Oklahoma that provides water to the residents of Pontotoc, Murray, Carter, Johnson, and Coal counties. Aquifer usage accounts for 63% of the public water supply in the area. The aquifer can be broken into a western and eastern side (Christenson et al., 2011). This thesis will focus on the Hunton anticline portion where BMS is located, called the Eastern Arbuckle-Simpson aquifer.

The aquifer has two major geologic sections: the Arbuckle Group and the Simpson Group. The Arbuckle Group is approximately a kilometer (3,000 feet) thick and consists of predominantly karstified dolomite. Water is stored in cavities, solution channels, fractures, and intercrystalline porosity. The Simpson Group overlies the Arbuckle Group and is generally less than 300 meters (1,000 feet) thick. It consists of sandstone, shale, and limestone. The Simpson Group is not present over the known BMS recharge area (Christenson et al., 2011).

.

The Eastern Arbuckle Simpson aquifer is structurally dominated by the Hunton Anticline. The Hunton Anticline formed during a period of uplift in the Pennsylvanian, generating fractures and folds (Christenson et al., 2011). BMS is located on the eastern edge of the Hunton Anticline along a major deformation zone called the Franks Fault (*Figure 3*).

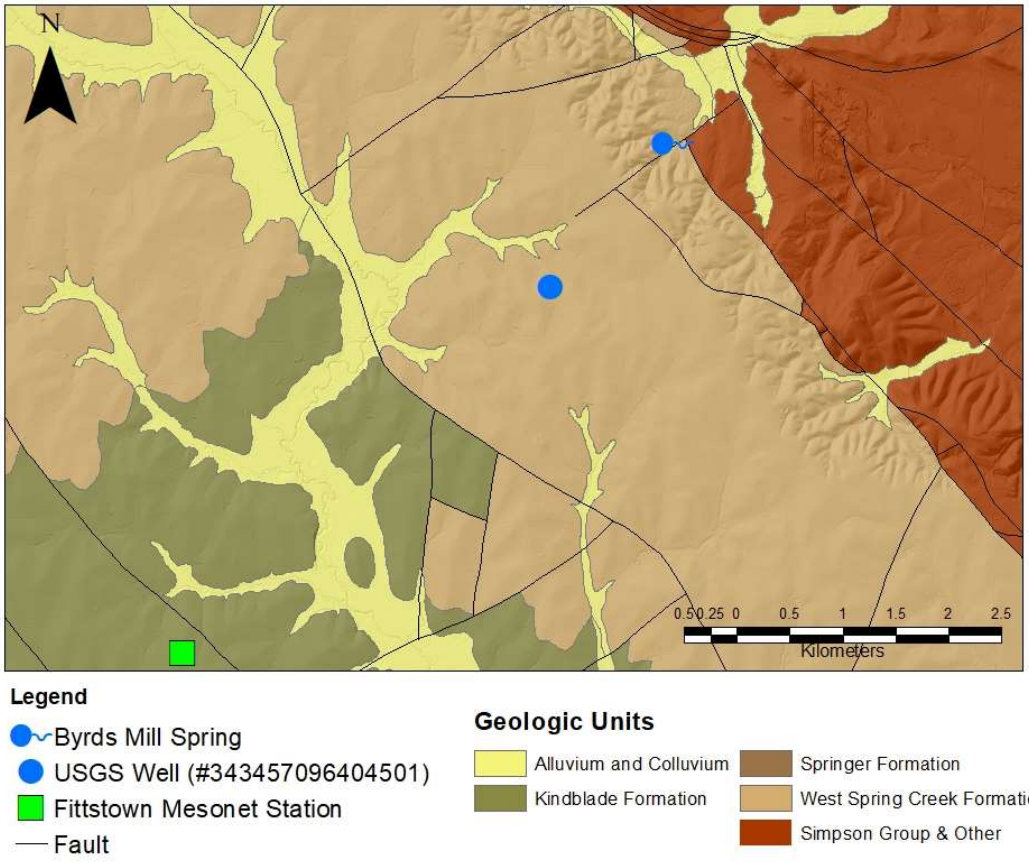

Figure 3: Geologic map of Hunton Anticline showing the location of BMS (Lidke and Blome, 2017)

The thickness of the Arbuckle-Simpson aquifer at the OWRB 89386/USGS Fittstown well located 1.7 km (1.1 mi) southwest of the spring is 1028 meters (3675 feet) (Rahi et al., 2009). The depth of the freshwater extent in the Arbuckle-Simpson aquifer is not known, but several deep wells drilled for the City of Ada in the formation near BMS produce freshwater below a depth of 300

meters (Christenson et al., 2011). Drill stem test results from wells drilled for petroleum in the Eastern Arbuckle-Simpson indicate that water is fresh at a depth of 559 meters (1,834 feet) (Puckette, 2009). Additionally, a USGS test well was drilled to a depth of 554 meters (1,820 feet), which produced meteoric freshwater (Christenson et al., 2011).

The Arbuckle-Simpson aquifer underwent a period of uplift and deformation during the Pennsylvanian orogeny that formed the Hunton Anticline. This mountain-building period resulted in the folding and faulting of Pennsylvanian and older strata (Christenson et al., 2011). Rivers and streams tend to run along these fault lines. In the northern portion of the Hunton Anticline, the dominant fault orientation is 115° (Halihan et al., 2009). Research has presented the possibility that BMS may be hydraulically connected to the largest stream in the aquifer, the Blue River, by the regional faulting. The northern portion of the Blue River is orientated at 115° but then turns south to 170°. If extrapolated, this 115° orientation creates a linear connection between the Blue River and BMS (Halihan et al., 2009).

BMS is located approximately 3.7 kilometers southwest of Fittstown, Oklahoma, and sits on the northeastern edge of the Eastern Arbuckle-Simpson aquifer (OWRB, 2007). BMS is located in the West Spring Creek Formation, a carbonate formation that is prone to fractures (Puckette, 2020; Musselman, 1994) The spring sits at the base of a plateau located to the west. There is a drop of approximately 40 meters in 0.6 kilometers from the edge of the plateau to the spring. The side of the plateau has been eroded into valleys by intermittent water flow. The spring is encased by a concrete structure held together by metal trusses. This structure was completed in 1927 to prevent the spring's discharge from becoming contaminated before flowing into a pipe that carries the water to the City of Ada, Oklahoma. The spring supplies the City of Ada and its ~17,000 residents with the majority of their water (Ada, 2020; OWRB, 2007).

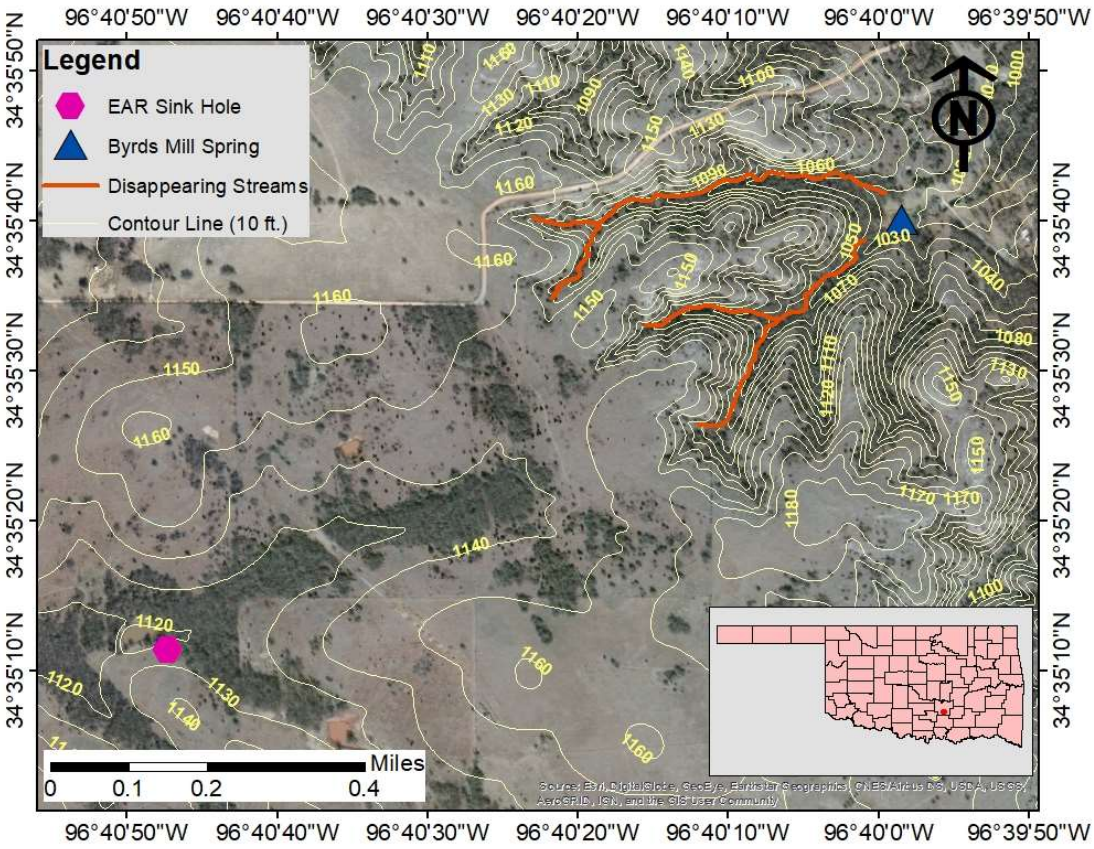

Figure 4: Location of Byrds Mill Spring and Surrounding Topography. Elevation values are feet and contour interval is 10 feet. Satellite image courtesy of ArcGIS (2020).

Hydrogeologic Setting

BMS sits on the eastern edge of the Hunton anticline where it discharges approximately 5% of the surface water discharge of the Eastern Arbuckle-Simpson aquifer. The spring discharges on average 0.5 cubic meters per second (cms) (18.5 cubic feet per second (cfs)) and is the largest spring in Oklahoma. The surface drainage basin (Figure 5) of the spring is only 0.5 km^2 which does not account for the large average discharge. An Oklahoma Water Resource Board study calculated that a much larger subsurface basin (*Figure 6*) of 140.35 km^2 supplies the spring with water (Christenson et al., 2011). The spring is interpreted as an underflow spring for the aquifer and has perennial flow (Halihan et al., 2009; Christenson et al., 2011). The perennial discharge of BMS

does not have extreme high flow events during storms, with discharge ranging between 0.19 cms (6.7 cfs) and 1.2 cms (40.0 cfs) in the historic record (1981 to 2016) (Stream gauging station: USGS 07334200 02N-06E-34 CCD 1 Byrds Mill Spring near Fittstown, OK – Peak Streamflow data set).

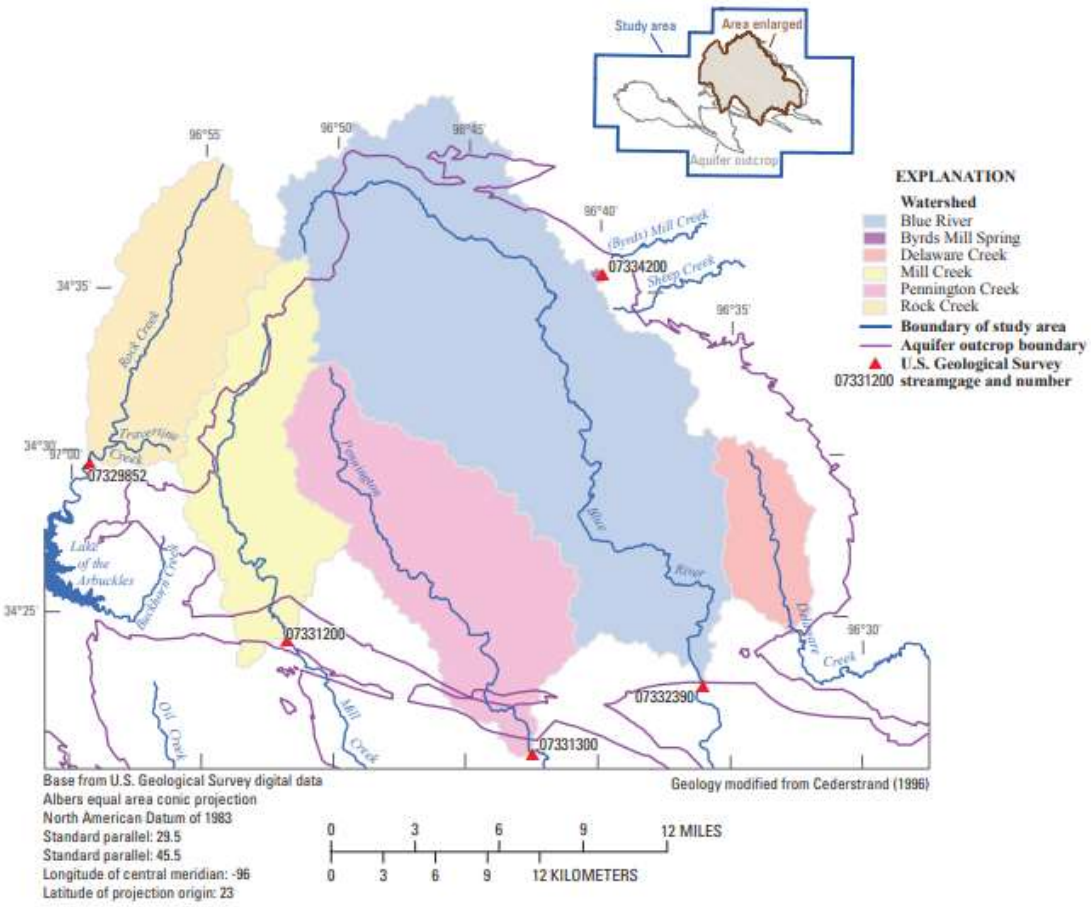

Figure 5: Surface watersheds in the Eastern Arbuckle-Simpson aquifer, south-central Oklahoma (from Christenson et al., 2011).

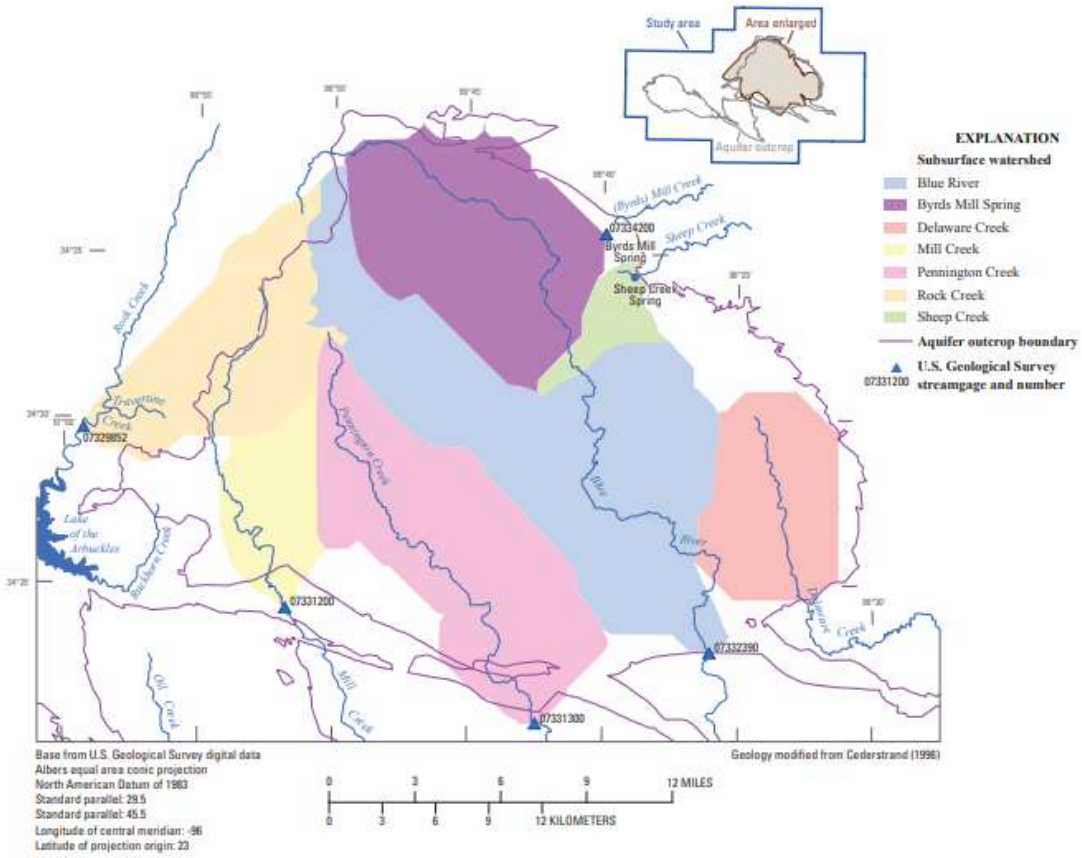

Figure 6: Subsurface watersheds in the Eastern Arbuckle-Simpson aquifer, south-central Oklahoma, based on synoptic water-level measurements (from Christenson et al., 2011).

Underflow springs are the lowest drainage points for an aquifer. Due to being located at the base of an aquifer, these springs are usually perennial. However, an underflow springs' flow is limited by the size of the discharge conduit. This is reflected in a spring's hydrograph, showing truncated high discharge peaks during storm events. Halihan and Mori (2009) demonstrated a relationship between the discharge of BMS and the discharge of Blue River and found the coefficient of determination (R^2) to be R^2=0.59. This relationship is what would be expected if BMS was acting as an underflow spring to the Blue River (Halihan et al., 2009).

In 2004, Christenson conducted a geochemical reconnaissance investigation of the Arbuckle-Simpson aquifer. Water samples were collected from 32 wells and springs across the aquifer. The analysis shows that water from the Arbuckle-Simpson aquifer is within the chemically appropriate range for all public supply uses. The concentration of dissolved solids was low with a median of 347 mg/L. The median of the specific conductance (electrical conductance) of the samples was 634 µS/cm and had a median pH of 6.9. (Christenson et al., 2011)

Several researchers have sampled BMS's specific conductance at different times. The results of these samples are in close proximity to each other. Between 2011 and 2012, Abongwa found that BMS's specific conductance was 419 µS/cm (Abongwa et al., 2018). Christenson found that BMS's specific conductance was 602 µS/cm on 11/10/2005 (Christenson et al., 2011).

The water temperature of springs in the Arbuckle-Simpson Aquifer is fairly constant (Swinea, 2012); the recharge water's residence time is long enough for the water temperature to equilibrate with rock temperature (Swinea, 2012). The shallow subsurface temperature of the Arbuckle-Simpson aquifer around BMS is between 18.0-18.5 °C (Swinea, 2012). BMS's water temperature is expected to reside around this range. A case study detailed in the OWRB's March 2007 newsletter recorded the water temperature of BMS as 18.3 °C (65 °F) (OWRB, 2007) and Christenson found that BMS's water temperature was 18.2 °C (64.7 °F) on 11/10/2005 (Christenson et al. 2009); confirming Swinea to be accurate. Slight variations do occur; Abongwa found that BMS's water temperature was 20.4 °C (68 °F) during his 2011-2012 study (Abongwa et al., 2018). This may be caused by the sample location within the spring.

BMS does not flow out of a cave or fissure; it bubbles up from a gravel filled pool (OWRB, 2007). Without an entry point, physical exploration of the spring cannot be performed; therefore, the conduit system of the spring is poorly understood. Geophysical surveys have been performed in the past (*Figure 7*) and suggest the conduit's geometry may consist of more than one flowpath

(Spears and Halihan, 2014). ERI data collected over BMS suggested that there were at least two flow paths into the spring. A large deep flow path was observed coming from depth along Franks Fault, which is believed to supply the spring with the majority of its water. A second shallower flow path was also observed in the ERI data along an interpreted bedding plane. This may provide a shallow path for siphon flow to affect the spring (*Figure 7*).

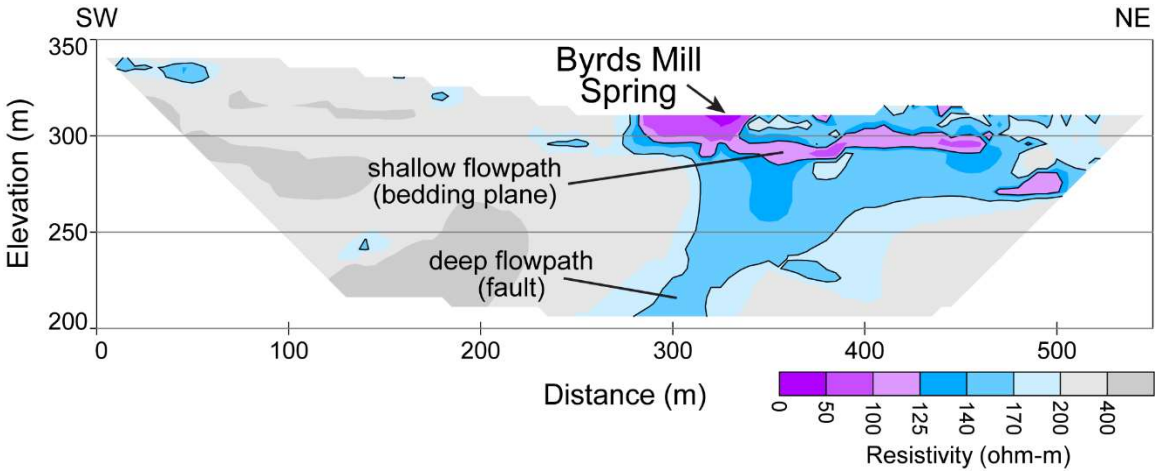

Figure 7: ERI of BMS showing shallow and deep flow paths.

Precipitation events have been shown to create a flashy response on karst springs hydrograph known as quickflow (Atkinson, 1977; Halihan and Wicks; 1998). Water from a storm event rapidly increases the spring's flow rate; once the slug of stormwater has passed the springs flow returns to the normal rate (Atkinson, 1977; Halihan and Wicks, 1998). This quickflow can cause large changes in the spring's water chemistry (Halihan and Wicks, 1998). As BMS is a karst spring, it may experience quickflow in water chemistry due to large precipitation events, even if the discharge pattern of an underflow spring doesn't allow a flashy discharge hydrograph.

CHAPTER IV

FIELD METHODOLOGY

EC reading were collected directly from BMS by an Oklahoma State University field team. All other data were collected from scientific databases provided by state and federal agencies.

Precipitation Data

Daily precipitation data were obtained from the Oklahoma Mesonet's Fittstown Station for a ten-year period from 2010 to 2020 to establish rainfall trends (Brock, 1995; McPherson, 2007). Monthly precipitation totals were collected for short term storm data for May 2015, during the monitored high storm period. The station is located 6.5 kilometers (4 miles) southwest of BMS (34.552050°, -96.717790°). The 10-year period used for precipitation data (January 2006 to December 2016) were plotted and analyzed to determine the average monthly precipitation and the precipitation amount for May 2015.

Spring Discharge Data

BMS discharge data were collected using a US Geological Survey (USGS) stream gauge (Gauge Number: USGS 07334200 02N-06E-34 CCD 1 Byrds Mill Spring nr Fittstown, OK). The USGS keeps records of monthly mean discharge and hourly discharge rates. The monthly mean discharge record for BMS is available for January 2006 to January 2017, and hourly discharge data were available for May 2015. The longer-term data set was plotted and analyzed to determine the average monthly discharge for the10-year period. This average discharge was compared to the discharge amounts for May 2015.

Groundwater Well Data

Daily water level data were retrieved from the Fittstown Well (*USGS Site Number: 343457096404501 - 01N-06E-04 CAD 1 Fittstown GW well)* for May 23, 2015 through May 25, 2015. The well is located approximately 1.7 kilometers (1.1 miles) southwest of BMS (34.582500°, -96.679167°). Head levels for the Fittstown Well were also collected from January 2010 to January 2017. These data were compared to the discharge records of BMS to establish a connection between groundwater elevation and discharge amount.

Electrical Conductivity Data

The spring fluid EC data were collected using a Hobo U24-001 electrical conductivity and temperature transducer (Onset Computer Corp.) placed inside the vault that covers Byrds Mill Spring. The transducer was placed at a spring orifice location, which exhibited large flow volumes referred to as Big Byrd Spring. This orifice comprises a large portion of the discharge measured by the USGS dataset. The Hobo U24-001 transducer was deployed and began collecting data on 11/24/14 at 12:00. The transducer was left in place, collecting electrical conductivity and temperature readings every 15 minutes until 3/8/2015 at 15:30. The transducer data file was downloaded and the transducer was redeployed on 5/23/2015 at 12:00, collecting EC and temperature readings every 15 minutes until 7/15/2015 at 15:30. This transducer data collection period recorded the extreme rainfall events that occurred in May of 2015.

CHAPTER V

FIELD RESULTS

Data sets were collected from an Oklahoma Mesonet station, a USGS groundwater well, and a USGS stream gauge. EC and temperature data were collected from a Hobo U24-001 transducer placed in BMS. The results are presented from the field data first to illustrate what the model is trying to replicate and what data were used to do so.

Precipitation Data

Precipitation data from the Fittstown Mesonet station shows that May 2015 is the wettest month on record from 2010 to 2020 (*Figure 8*). The average monthly rainfall for the 10-year period is 3.53 inches; in May of 2015, the station recorded 22.44 inches of rain (*Figure 9*). This is more than six times the monthly average for the 10-year period.

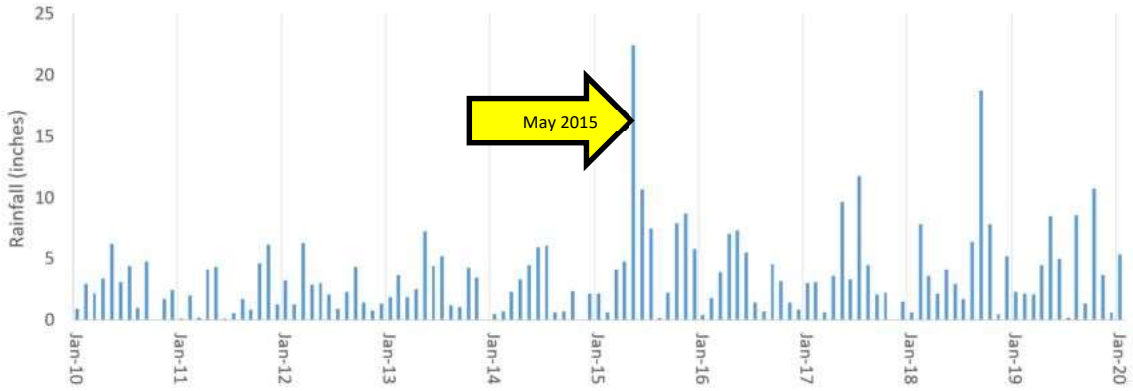

Figure 8: Ten years of monthly rainfall amounts (2010 to 2020) from the Fittstown Mesonet station.

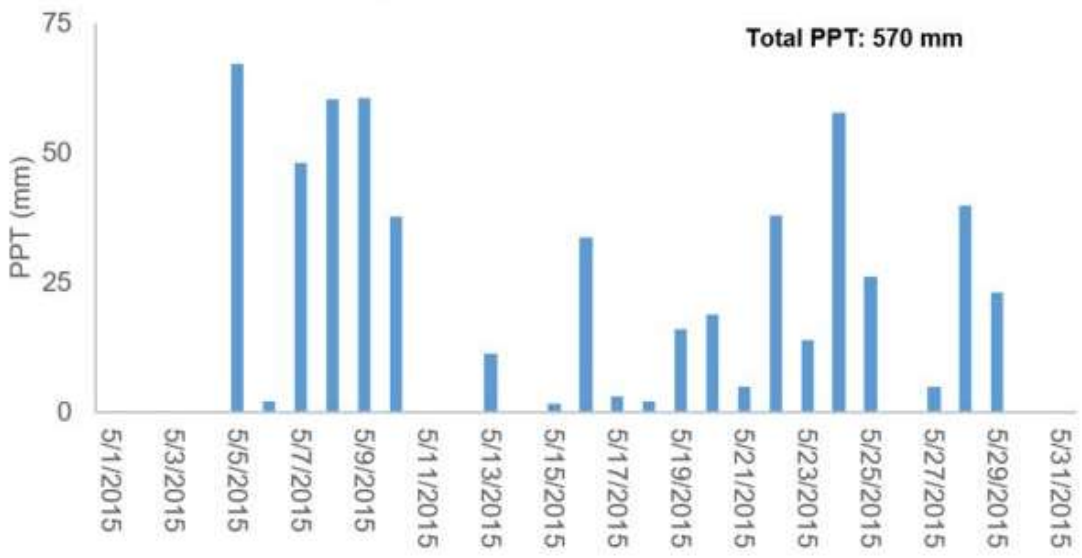

Figure 9: Daily precipitation totals for May 2015 for the Fittstown Mesonet Station.

Groundwater Well Data

Average monthly groundwater elevations from the USGS Fittstown groundwater were collected from January 2010 to January 2017. The collected groundwater elevation data show that May 2015 head levels were well above average (*Figure 10).*

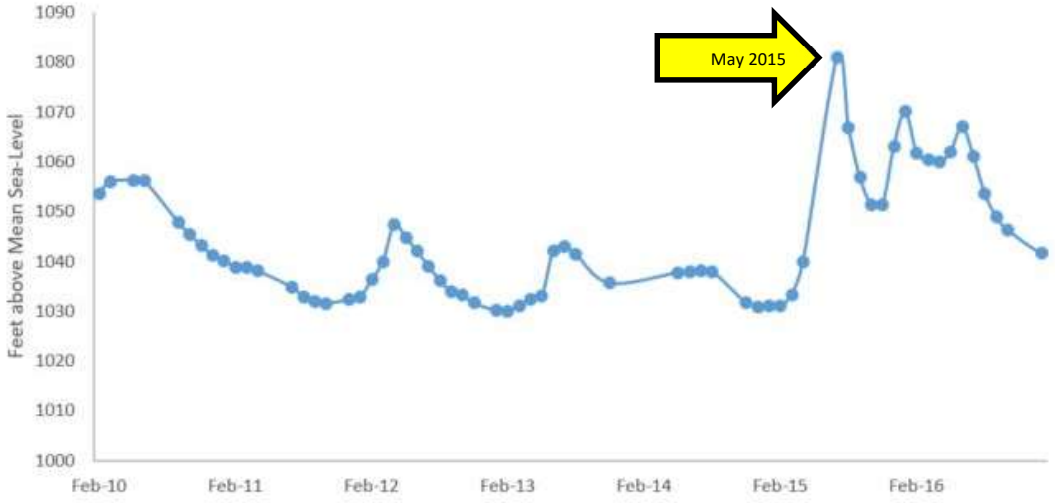

Figure 10: Average monthly groundwater elevations for the USGS Fitstown groundwater well (#343457096404501).

Daily groundwater elevations were collected for the 48-hour period of interest on the EC chemographs, May 23 to May 25, 2015 (Table 1). These data points were used as the head levels to calculating discharge for the regional aquifer model.

Table 1: USGS Fitstown Groundwater Well Water Level			
Date	DTW (ft)	Casing Elevation (ft)	Water elevation from Sea Level (m)
5/23/2015	84.48	1155.00	326
5/24/2015	81.93	1155.00	327
5/25/2015	78.58	1155.00	328

Spring Discharge Data

Discharge data from the USGS stream gauge at BMS (USGS 07334200 02N-06E-34 CCD 1 Byrds Mill Spring nr Fittstown, OK) shows that BMS experienced a higher than average discharge in May 2015 (*Figure 10*). The average monthly discharge for the spring from 2006 to 2016 (the USGS ceased data collection in January 2017) is 0.27 cms (9.43 cfs). The discharge for the 5/23/2015 to 5/25/2015, the period of interest, is between 0.85 cms (30 cfs) and 1.13 cms (40 cfs) (*Figure 12*). This is more than three times the monthly average for the 10-year period.

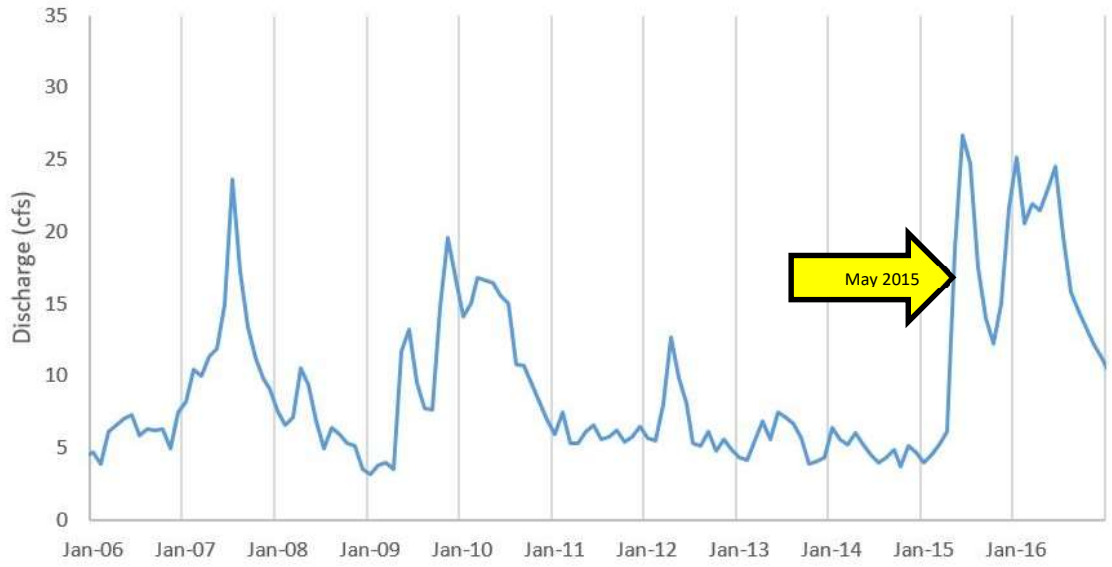

Figure 11: BMS Monthly Average Discharge from 2006 to 2016.

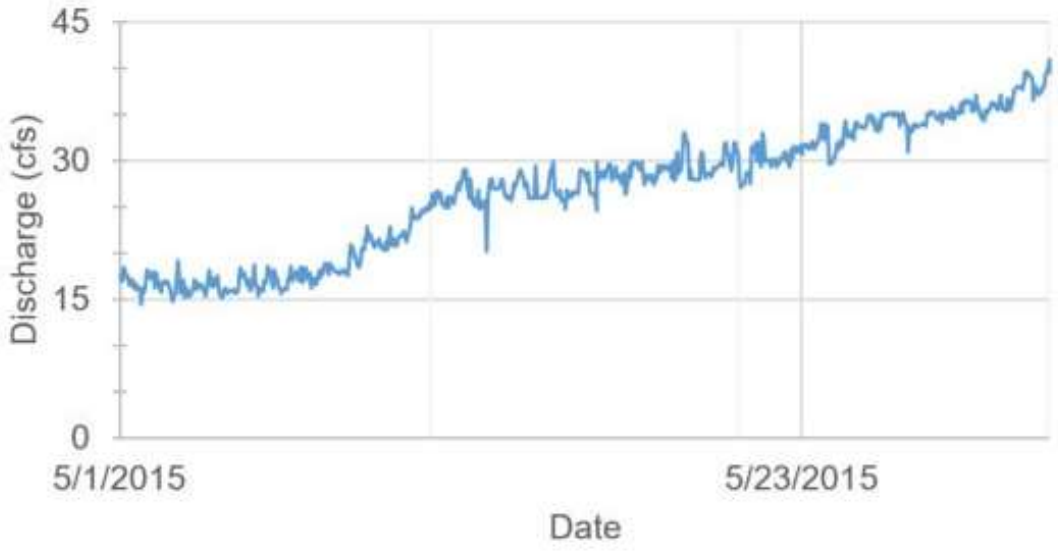

Figure 12: BMS Discharge for May 2015.

Discharge data from BMS was statistically compared to head levels of the Arbuckle-Simpson aquifer taken from the USGS Fittstown groundwater well (#343457096404501). A strong correlation between the head levels and discharge was observed (R^2=0.91) (*Figure 13*). Because this relationship is so strong, USGS groundwater well head levels were used to calculate the discharge rate of modeled Regional Aquifer flow.

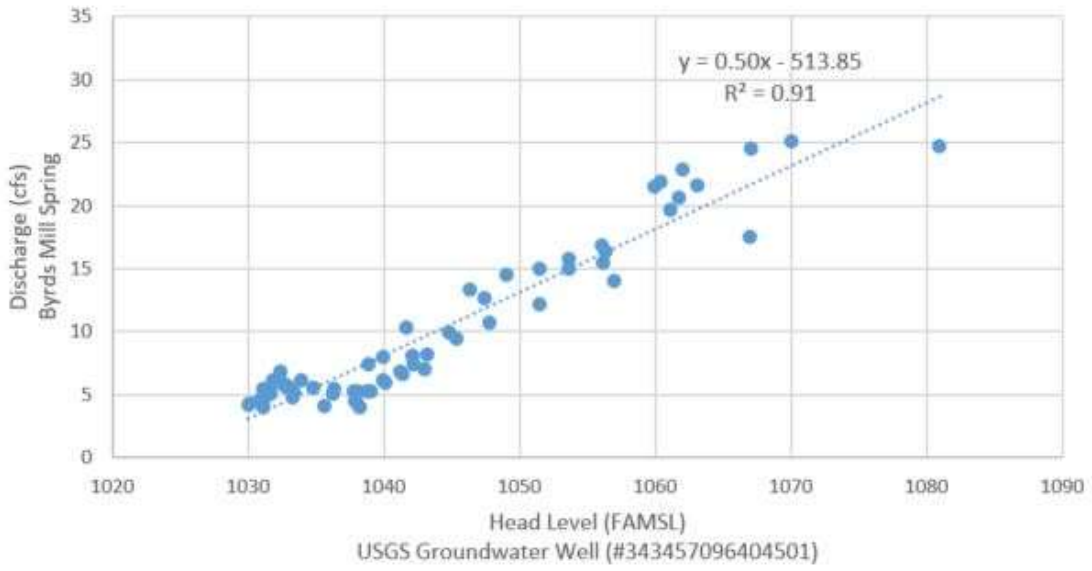

Figure 13: Relationship between the head level of the USGS Fittstown groundwater well (#343457096404501) and the discharge of BMS.

Electrical Conductivity Data

In March of 2015, extreme levels of precipitation occurred in the spring's basin. EC data were collected from BMS. Prior to the storm events, data shows that BMS exhibited stable fluid EC when at baseflow. The extreme rain events of May 2015 caused BMS to fall out of equilibrium. During the storm event, data loggers recorded EC levels of the discharged water dip to approximate 10 µS/cm and then return to the aquifer water's equilibrium EC of 520 µS/cm approximately 16 times in a 48-hour period (Figure 18). This is indicative of pure rainwater discharging from the spring.

Prior to the March 2015 precipitation events, baseflow fluid EC data were collected. When at baseflow, the electrical conductivity (EC) of the water discharging from BMS averages 520 µS/cm with little variation. Four months (11/24/2014 to 3/8/2015) of EC data collected from BMS shows that the baseflow only varied by +/- 4 µS/cm.

During the May 2015 precipitation events, the stormwater chemistry of BMS began to oscillate. The collected transducer data revealed an oscillation in the fluid EC between ~520 µS/cm and ~10

µS/cm (*Figure 14*). Based on the fluid EC of average rainwater, when the EC decreases to ~10 µS/cm the springs discharge is interpreted as 100% rainwater.

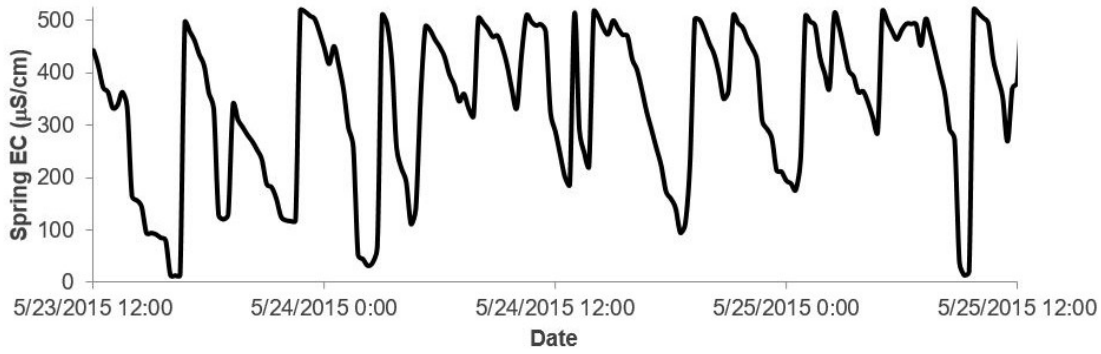

Figure 14: Storm Event Spring Electrical Conductivity for BMS.

Electrical Conductivity vs Discharge Data

The collected EC data's oscillations did not correlate to any changes in discharge collected from the USGS gauging station. A comparison of BMS' EC and discharge shows very little correlation (Figure 15). EC oscillated approximately every two hours. The discharge of BMS's trended upward, and while there was some oscillation in the BMS' discharge, it did not correlate statistically with BMS' EC ($R^2 = 0.09$).

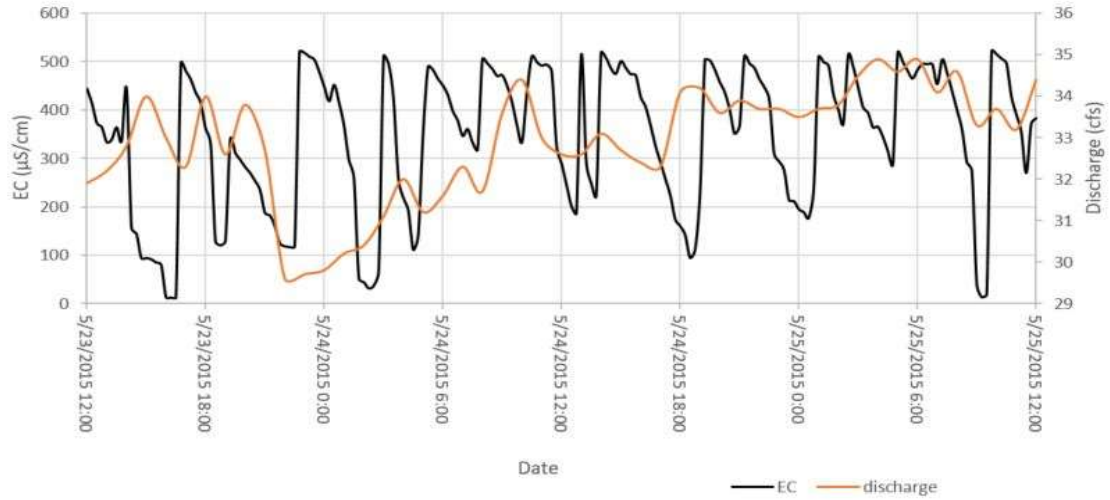

Figure 15: BMS' field EC vs discharge.

CHAPTER VI

MODEL PROCESSES

Numerical models of the fluid EC response of the spring over time (EC chemographs) of BMS were created in Excel to test the field data collected from BMS and determine if the siphon hypothesis could explain the pattern presented by the field data. Analytical solutions were used to simulate what the EC chemographs would be for a set of four siphon and mixing processes expected to affect the EC of the spring. The sections below describe how the numerical model was constructed, how the model was calibrated, and the results of that model.

The general BMS system was conceptualized as a set of tanks with drains (Figure 16). The Siphon-Tank represents a local karst recharge features present on intermittent stream beds upgradient of the spring that enters the shallow portion of the aquifer. The Regional-Tank represents the primary deep regional flow system of the Eastern Arbuckle-Simpson aquifer. The tanks are connected by a series of pipes to represent the flow paths that connect the local recharge features, the regional aquifer, and the BMS orifices. The Siphon-Tank's drain pipe forms a hydraulic siphon and only discharges water when head levels in the Siphon-Tank are high enough. The Regional-Tank's drain pipe flows continuously toward the simulated outflow representing BMS spring. The two pipes meet at a T-junction where mixing occurs between the local and regional flows. The water from both tanks discharges from a single pipe that represents BMS. The Siphon-Tank local flow, the

Regional-Tank regional flow, and the two mixing processes, one in the Siphon-Tank and the other between the local and regional flow will be discussed in detail in the subsequent sections.

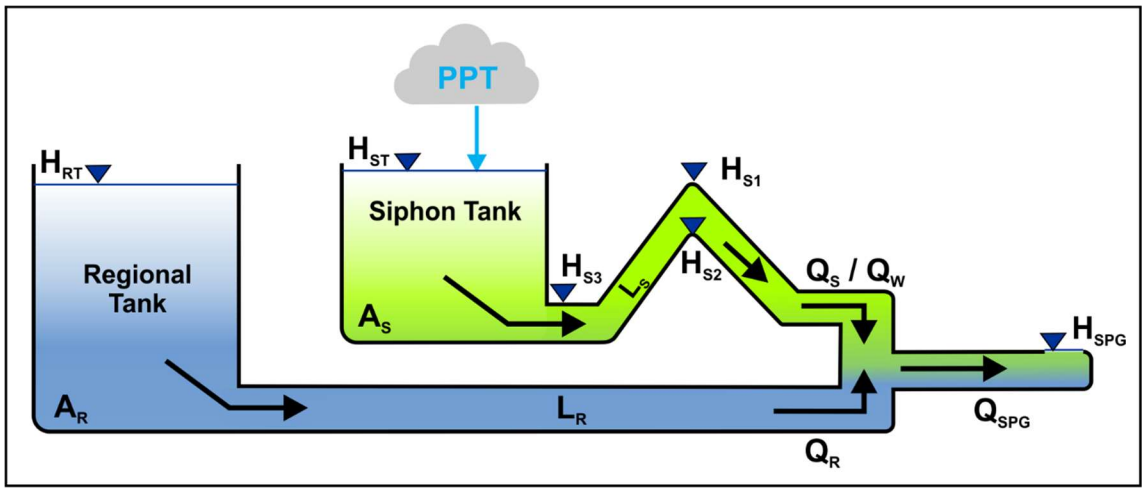

Figure 16: Visualization of Model – Regional-Tank and Siphon-Tank are connected to BMS by a T-junction.

Model calibration was performed for each section of the overall model. Pre-siphon mixing is calibrated by increasing or decreasing the precipitation flow rate and/or equilibrium aquifer water content of the Siphon-Tank. The siphon and the adjoining tank were calibrated by taking known values of real-world karst features in the surrounding area and calculating the unknown values that simulated the system. T-junction mixing is calibrated by determining which type of flow best simulated the field data. The regional aquifer flow is calibrated by matching real-world aquifer head and distance conditions to the spring flow rate.

Regional Aquifer Model

A numerical model was created to simulate the stable baseflow of BMS. Flow was modeled as straight pipe flow. The model used the regional aquifers' head levels measure at a nearby well to calculate the discharge of the modeled spring.

Numerical Model

Regional aquifer flow ($Q_{Regional}$) was modeled to create a data set of base flow rates and associated EC data. The model simulates how BMS's baseflow discharge is affected by the regional Arbuckle-Simpson aquifer. The regional aquifer flow model was only used to determine changes in the discharge rate of the spring. The EC of the Arbuckle-Simpson aquifer is stable with low variability (Christenson et al. 2009; Swinea, 2012; Abongwa et al., 2018), so EC was set at a constant 520 µS/cm for the regional system. Discharge from the aquifer is characterized by Equation (7) as a tank with normal (non-siphoning) pipe drain model (Halihan and Wicks, 1998; Turcotte et al. 2002).

$$Q_{Regional} = -4.706\,\pi\,\frac{g^{4/7}}{V^{1/7}}\,R_{Regional}^{19/7}\left(\frac{\Delta h}{L_{Regional}}\right)^{4/7} \quad (7)$$

where $Q_{Regional}$ is the discharge from Arbuckle-Simpson Aquifer/Regional-Tank's drainage pipe (cms), g is the gravitational constant (m/s^2), V is the kinematic viscosity of the fluid (m^2/s), $R_{Regional}$ is the radius of the drainpipe (m^2), $L_{Regional}$ is the length of the drainpipe (m), and Δh is the difference in water level on either side of the pipe (m).

Model Calibration

Long-term groundwater elevation data (2010 to 2017) from the USGS well (#343457096404501) were compared to long-term BMS discharge. Statistical analysis was performed and determined a high degree of correlation exists between the Arbuckle-Simpson's groundwater elevation and BMS's discharge. The relationship between the hydraulic gradient from the well to the spring and spring discharge was utilized for the analytical model.

The actual length of the aquifer's drain-pipe is unknown, therefore the distance from the USGS Fittstown well to BMS is used. $R_{Regional}$ was determined by back calculating from the USGS average

discharge field measurements of BMS during the time period. These variables were used to determine the regional discharge from the aquifer.

The following values were used in conjunction with the head values from the relationship between the hydraulic gradient from the well to the spring and spring discharge was utilized for the analytical used in combination with the following parameters to complete *Equation* (7) to produce the regional aquifer discharge:

$g = 9.807\ m/s^2$;

$v = 1.0445 \times 10^{-6}\ m^2/s$ (Kestin et al., 1978; Crittenden et al., 2012);

$R_{Regional} = 0.20$ m;

$L_{Regional} = 1772$ m;

Δh = Table 1 values - 313 m.

For the Pre-Siphon mixing, half of the Siphon-Tank is filled with equilibrium aquifer water with an EC of 520 µS/cm. precipitation is then added to the Siphon-Tank at a rate of 473 liters (125 gallons) per second.

Model Results

The Arbuckle-Simpson regional aquifer is constantly discharging out of BMS, except when interrupted by large flows of siphon discharge. Based on the data taken from the USGS well *(Site Number: 343457096404501 - 01N-06E-04 CAD 1 Fittstown GW well)* for May 23, 2015 through May 25, 2015 the water level of the aquifer rose each day. This rise in head level caused the aquifer to discharge more water each day. In reality, the water level most likely rose gradually, but only one measurement of head conditions was available for each day in question. The fluid EC pattern would not change as the regional model included a constant fluid EC value of 520 µS/cm.

Siphon Tank Model

A siphon model was created to simulate siphon flow from a localized karst flow path. The model pipe that drains the Siphon-Tank forms a siphon and only discharges water when head levels in the

Siphon-Tank (H_{ST}) are high enough (greater than H_{S2}) (*Figure 16*). The Siphon-Tank has a uniform basal area (A_S), with an outlet head level of H_{S3}.

Numerical Model

The Siphon-Tank discharge is primarily controlled by head levels in the Siphon-Tank and whether the tank is filling or draining (*Figure 17*). The siphon is turned on and off by the head level inside the Siphon-Tank compared to the elevation of the siphon structure. Water from the surface (Q_{PPT}) enters the Siphon-Tank raising the head level (H_{ST}). When the Siphon-Tank's head level (H_{ST}) rises to the bottom of the drain pipe's crest (H_{S2}), water spills over the top, and weir flow (Q_W) begins to flow towards the spring (H_{SPG}). If the Siphon-Tank's head levels continue to rise to the top of the siphon's crest (H_{S1}), the siphon becomes primed and siphon flow (Q_S) begins to flow to towards the spring (H_{SPG}). Siphon flow (Q_S) will continue until the Siphon-Tank drains below the siphon pipe's entrance (H_{S3}). When the Siphon-Tank's head levels (H_{ST}) drop to below the siphon pipe's entrance (H_{S3}) air will enter the siphon pipe unpriming it, and causing flow to cease (*Figure 17*).

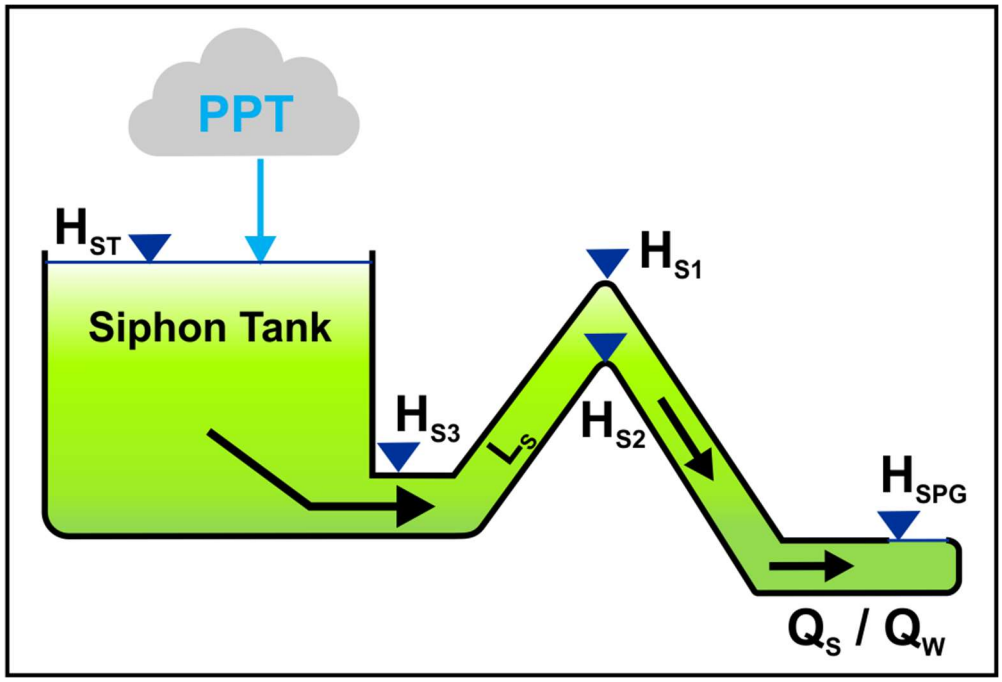

Figure 17: Siphon Structure – Precipitation enters the Siphon-Tank raising HST. When HST rises to HS2, weir flow (QW) begins to flow to HSPG. When HST rises to HS1, siphon flow (QS) begins to flow to HSPG, which drains the Siphon-Tank. QS ceases when HST drops to HS3 and siphon flow ceases.

As surface water enters the Siphon-Tank (Q_{PPT}) it increases the head level in the Siphon-Tank (H_{ST}). When the head level in the Siphon-Tank (H_{ST}) reaches the height of the bottom of the siphon pipes crest (H_{S2}) water will flow through the model pipe as a weir system and flow out of the siphon pipe (Q_{Weir}). Flow over the weir is controlled by parameters accounted for in *Equation* (8) (Bonacci and Bojanić, 1991).

$$Q_{wier}(t) = 0.42 * B * 2g^{½}(H_{ST}(t) - H_{S2})^{1.5} \quad (8)$$

where $Q_{Wier}(t)$ is the discharge of siphon pipe from weir flow at time t (seconds), 0.42 is the overflow discharge coefficient (dimensionless), B is the weir overflow discharge width (≤ of the pipe diameter) (meters), and g is the gravitational constant.

If the flow rate of precipitation into the Siphon-Tank (Q_{PPT}) is greater than weir flow (Q_{Weir}), the head level in the Siphon-Tank (H_{ST}) will continue to rise. When the head level in the Siphon-Tank (H_{ST}) increases to the top of the siphon pipe's crest (H_{S1}) the siphon will be primed and begin to

flow (Q_{Siphon}) according to the fluid dynamics of siphons represented by Equation (9) (Bonacci and Bojanić, 1991):

$$Q_{siphon}(t) = \frac{d_s^{\,2}\,\pi}{4} \frac{[2g(H_{ST}(t) - H_{SPG})]^{½}}{[1 + \xi_u + \lambda_s l_s / d_s]^{½}} \quad (9)$$

where $Q_{Siphon}(t)$ is the discharge of siphon pipe from siphon flow at time, t *(cms)*, d_s is the siphon pipe diameter (meters), l_1 is the siphon pipe length (meters), H_{SPG} is the height of the siphon pipe exit at the spring (meters), $\mathcal{E}_u$ is the coefficient of the energy loss at the siphon pipe entrance (= 0.5), and λ_s is the friction coefficient in the siphon pipe. The friction coefficient was determined by using the Colbrook-White equation.

The head level in the Siphon-Tank (H_{ST}) must be calculated for each time step to compute Equation (8) and (9). Discharge leaving the siphon pipe ($Q_{Siphon/Weir}$) lowers head in the Siphon-Tank (H_{ST}). Perception coming in the Siphon-Tank (Q_{PPT}) raises the head in the Siphon-Tank (H_{ST}). The head in the Siphon-Tank (H_{ST}) at time(t) can be calculated by:

$$\Delta H_{Rise}(t) = \frac{Q_{PPT}(t)}{\text{Tank Area}} \quad (10)$$

$$\Delta H_{Fall}(t) = \frac{-Q_{S/W}(t)}{\text{Tank Area}} \quad (11)$$

$$\Delta H_{st}(t) = \Delta H_{Rise}(t) + \Delta H_{Fall}(t) + H_{ST}(t-1) \quad (12)$$

Where $\Delta H_{Rise}\ (t)$ is the rise in head at time (t) (m), $Q_{PPT}\ (t)$ in the inflow of precipitation into the tank at time (t) (m^3), *Tank Area* is the length times the width of the Siphon-Tank (m^2), $\Delta H_{Fall}\ (t)$ is the fall in head at time (t) (m), $Q_{S/W}\ (t)$ in the discharge out of the Siphon-Tank at time (t) (m^3),

$\Delta H_{ST}\ (t)$ is the head level of the Siphon-Tank at time (t) (m), and $H_{ST}\ (t\text{-}1)$ is the head level in the Siphon-Tank at the previous time step ($t\text{-}1$) (m).

If siphon flow (Q_{Siphon}) is greater than the amount of precipitation entering the Siphon-Tank (Q_{PPT}) the tank begins to drain. The siphon continues to flow until the head level in the Siphon-Tank (H_{ST}) drops to below the top of the siphon pipe entrance (H_{S3}). When this occurs air becomes entrained in the pipe, the siphon becomes unprimed, and the flow ceases (Bonacci and Bojanić, 1991).

The friction coefficient in the siphon pipe (λ_s) must be found to complete Equation (9). The friction coefficient will vary with the size of the siphon pipe. The friction coefficient in the siphon pipe (λ_s) is determined by the Colbrook-White equation (Equation (13)) (Evett and Liu, 1989).

$$\frac{1}{\sqrt{\lambda}} = -2\log\left(\frac{k_s}{3.7D} + \frac{2.51}{RE\sqrt{\lambda}}\right) \tag{13}$$

Where D is the density of the fluid (kg/m^3), K_s is the pipe roughness factor, λ is the friction coefficient, and RE is the Reynold's Number (Kg/mPa*s2).

The Reynold's Number (RE) must be found to complete Colbrook-White equation. The Reynold's number is determined using Equation (14) (Evett and Liu, 1989).

$$RE = \frac{\rho * V * A}{\eta} \tag{14}$$

where RE is the Reynold's Number, ρ is the density of the fluid, V is the velocity of flowing liquid (m/s), A is the cross-sectional area of the pipe (m^2), and η is the viscosity of the fluid at a certain temperature (kg/m*s).

Model Calibration

The siphon portion of the model was broken into two categories for calibration purposes: the siphon pipe and the siphon's adjoining tank. The siphon model was calibrated by combining real-world conditions with probable values to determine the siphon's and corresponding tank's physical properties. The siphon pipe's length was calibrated by hand, manually adjusting the input in the model.

Since a discharge correlation between BMS and the Blue River had been shown in previous reports, the first input was the distance between these two objects. The pipe diameter and corresponding friction coefficient were then calculated using Excel's Goal Seek to determine if the correct amount of discharge could be produced with the siphon connected to the Blue River. The discharge of the model was calculated to match the field measurements. When calibrated at this distance the diameter of the modeled drain would be too large to fit with expected cave or fracture sizes in the Arbuckle-Simpson aquifer. Next, the model was run using the distance between the EAR Site sinkhole and BMS, but due to the distance from the EAR site to BMS, the pipe size was too large for caves or fractures observed in the Arbuckle-Simpson Aquifer. Because the Blue River and the EAR sinkhole were located too far away, pipe lengths that fell between the EAR site and BMS were tested with the model. The calibrated model indicated that the siphon would be within 100 meters from the site.

Once the siphon pipe's dimensions were calibrated, the tank size could be calibrated. The Siphon-Tank's height has to be greater or equal to H_{S1}-H_{S3}+d_1. The length and width of the Siphon-Tank were manually calibrated to recreate the number of EC oscillations observed in the field data. The Siphon-Tank size must also correspond with the inflow rate of precipitation. The precipitation inflow rate can be changed manually to produce the correct amount of oscillations observed in the field data in accordance with a certain size of the tank. If the precipitation inflow rate is known,

precipitation can also be set as a constant and the tank size can be changed to match the observed field oscillations.

Model Results:

There are three major patterns that occur for the siphon discharge, based on the input and output of the Siphon-Tank. If the discharge of the siphon (Q_{weir}) is less than the incoming precipitation (Q_{PPT}), there will be flow over the weir but the siphon will never prime. If the incoming precipitation amount is greater than the weir and siphon discharge, the siphon will prime but will never stop flowing. Finally, if the incoming precipitation amount is between the weir and siphon discharge rates, the siphon will prime, drain the Siphon-Tank, and unprime.

If $Q_{Weir} < Q_{PPT} > Q_{Siphon}$ occurs then the discharge hydrograph will form an oscillating pattern due to the Siphon-Tank repeatedly filling and draining (*Figure 18*). As precipitation enters the Siphon-Tank (Q_{PPT}), water levels rise to H_{S2}, triggering weir flow (Q_{Weir}). If the rate of precipitation entering the tank is greater than Q_{Weir} the head levels in the Siphon-Tank continue to rise to H_{S1}, priming the siphon and activating siphon flow (Q_{Siphon}). If Q_{Siphon} is greater than Q_{PPT} the head level will lower to H_{S3} ceasing Q_{Siphon}. This process will repeat as long as Q_{PPT} rates remain within this range.

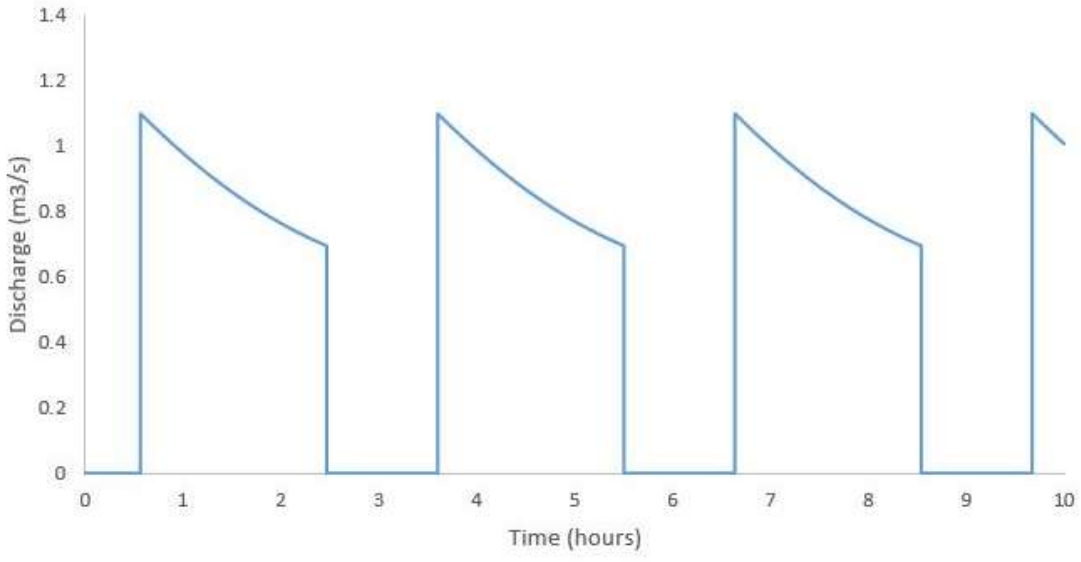

Figure 18: $Q_{Weir} < Q_{PPT} > Q_{Siphon}$ – Siphon Discharge

If $Q_{PPT} > Q_{Weir}$ & $Q_{Siphon\text{-}Min}$ (the minimum siphon discharge) occurs then the discharge will form the graph shown in *Figure 19*. There is no repeating oscillation on the discharge graphs; the discharge rate rises rapidly and then drops. Following the drop, the discharge rate and head level remain constant. This pattern occurs because the head level in Siphon-Tank never falls below H_{S3} so the siphon remains operational.

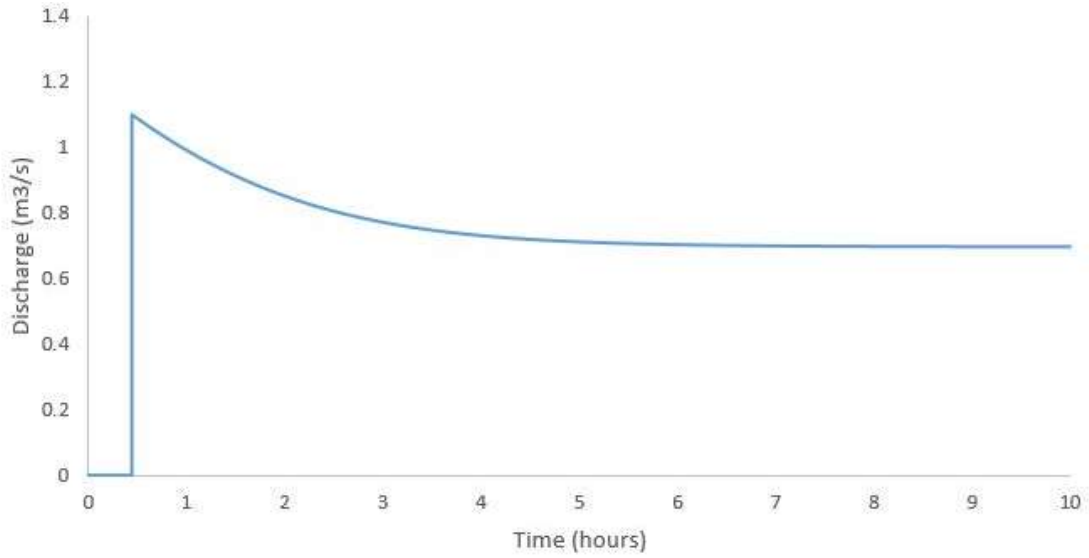

Figure 19 : $Q_{PPT} > Q_{Weir}$ & $Q_{Siphon\text{-}Min}$ - Siphon Discharge

If $Q_{PPT} > Q_{Weir}$ & $Q_{Siphon\text{-}Max}$ (the maximum siphon discharge) occurs then the discharge will form the graphs shown in *Figure 20*. There is no repeating oscillation on discharge graphs. The discharge rate rises rapidly and stays high. This pattern occurs because the head level in Siphon-Tank never falls below H_{S3} so the siphon remains operational.

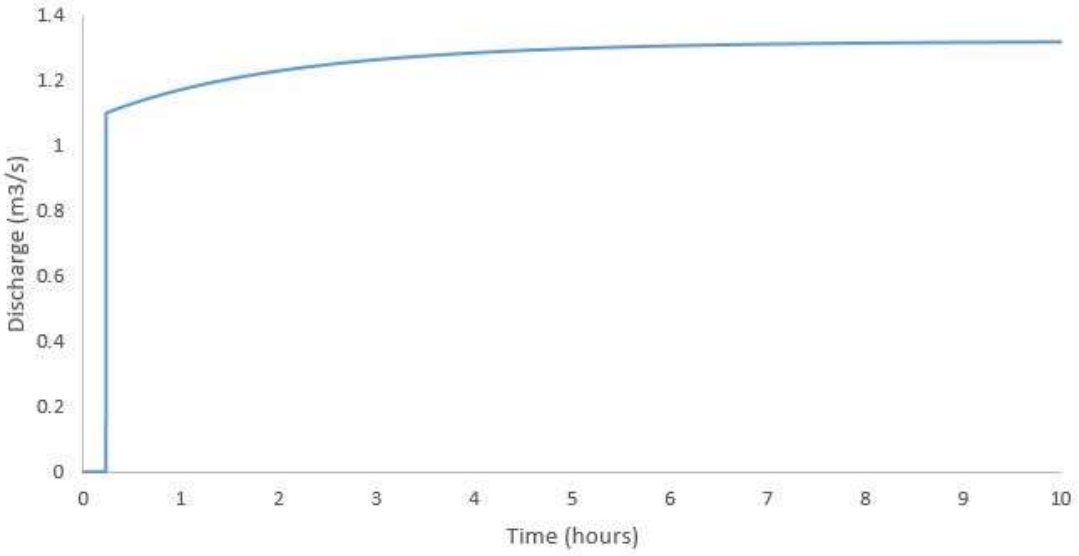

Figure 20 : $Q_{PPT} > Q_{Weir}$ & $Q_{Siphon\text{-}Max}$ - Siphon Discharge

If $Q_{PPT} < Q_{Weir}$ occurs then the discharge will form the graph shown in *Figure 21*. There is no repeating oscillation on the discharge graph; the discharge rate rises rapidly and levels out. This happens because the head level in Siphon-Tank never rises to H_{S1} and the siphon does not become primed. Because the siphon is never activated, Siphon-Tank can never fully drain.

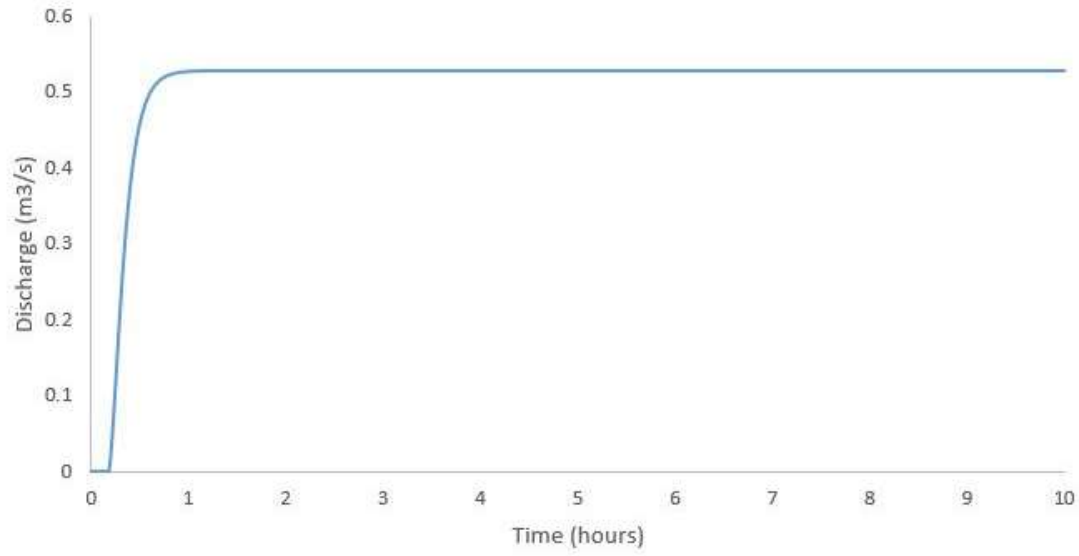

Figure 21: $Q_{PPT} < Q_{Weir}$ - Siphon Discharge

Siphon discharge is controlled by the head level in the Siphon-Tank. The head level is raised by precipitation flowing into the Siphon-Tank; the head level is lowered by weir and/or siphon discharge. Several different discharge patterns occur when rainfall enters Siphon-Tank, depending on inflow amounts. Precipitation must flow into the Siphon-Tank at the correct rate for the siphon to produce an oscillating discharge. If the correct rate of precipitation does not enter the Siphon-Tank, oscillation in siphon discharge will not occur.

T-junction Mixing

A model was created to mix the variable EC discharge from the Siphon-Tank and the stable EC discharge from the Regional-Tank. Simulated water from the Siphon Tank and the Regional Aquifer Tank meet at the T-Junction and flow out of one pipe (the spring). The model simulates how water from the Siphon-Tank and the Regional-Tank meets at a T-junction, mixes, and discharges to BMS.

Numerical Model

Continuous and discontinuous flow mixing is described in Chapter II. Because the spring fluid EC data suggests that BMS's discharge consists entirely of precipitation at some time intervals, the flow is simulated as continuous flow properties. There are two types of continuous flow. Due to BMS being interpreted as an underflow spring the continuous flow equation where the outflow is less than the inflow Equation (15) was used. Flow through the T-junction is mathematically represented by *Equation* (15), which was derived from *Equation* (3) (Johnson et al., 2006).

$$C_{SPG} = C_{ST}\left(\frac{Q_{ST}}{Q_{SPG}}\right) + C_R\left(1 - \frac{Q_{ST}}{Q_{SPG}}\right) \quad (15)$$

where C_{SPG} is the EC of the spring's discharge (µS/cm), $C_{Siphon\text{-}Tank}$ is the EC of the Siphon-Tank's discharge (µS/cm), $C_{Regional\text{-}Tank}$ is the EC of the Regional-Tank's discharge (µS/cm), $Q_{Siphon\text{-}Tank}$, is the discharge rate of the Siphon-Tank (cms), $Q_{Regional\text{-}Tank}$ is the discharge rate of the Regional-Tank (cms).

The groundwater mixing ratio is dependent on how much water is flowing from the Siphon-Tank into the T-junction. When water levels in the Siphon-Tank are below the bottom of the siphon pipe (H_2), only discharge from the Regional-Tank flows into the junction and no mixing occurs (*Figure 22*a). As head levels in the Siphon-Tank rise to generate weir flow, the weir flow mixes with the discharge from the Regional-Tank and lowers the EC of the water discharging from the spring (*Figure 22*b). When head levels in the Siphon-Tank rise above the top of the siphon pipe (H_{S1}), the siphon becomes primed and begins to flow. The siphon flow mixes with water flowing from Regional-Tank (*Figure 22*c). Eventually, the siphon flow overwhelms the flow from the Regional-Tank, lowering the EC of the water discharging from the spring to the EC of the Siphon-Tank (*Figure 22*d) (Park and Lee, 1999; Johnson et al., 2006).

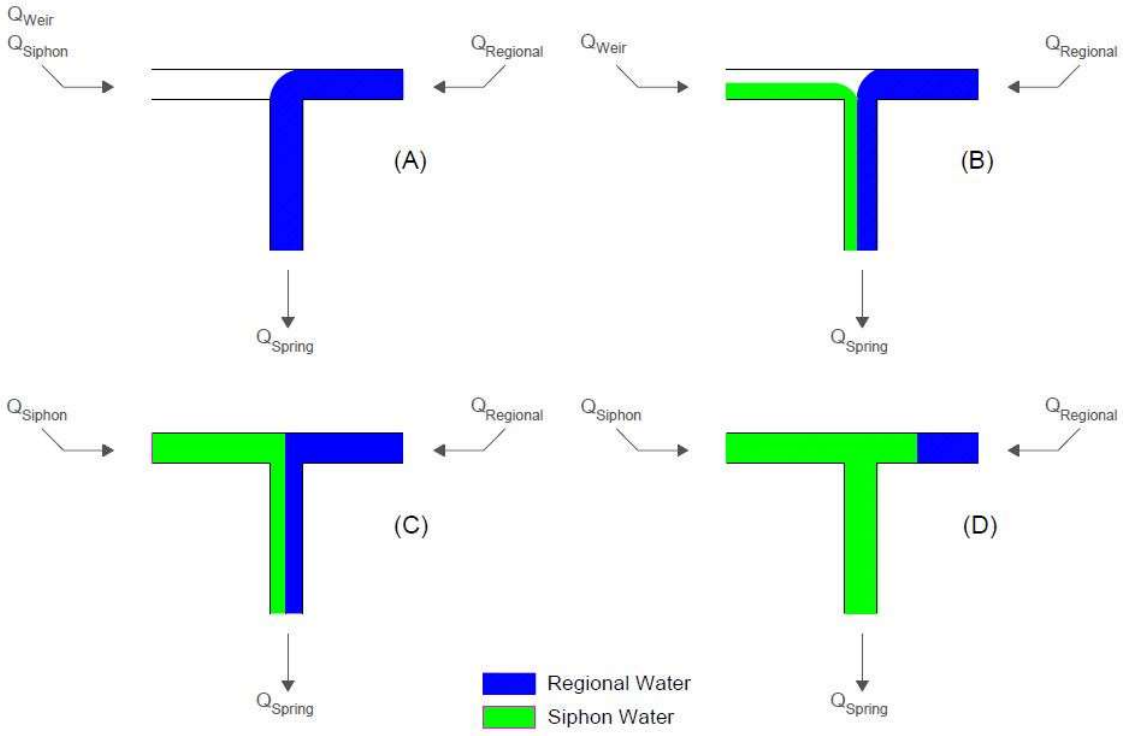

Figure 22: T-Junction Mixing – (A) Inactive siphon, only discharge at the spring is from the Regional-Tank; no mixing occurs; (B) Weir flow from the Siphon-Tank mixes with the discharge from the Regional-Tank; (C) Siphon flow from the Siphon-Tank mixes with the discharge from the Regional-Tank; (D) Siphon flow from the Siphon-Tank overwhelms the discharge of the Regional-Tank resulting in pure siphon discharge at the spring.

Calibration

BMS is an underflow spring, therefore the spring's inflow should be more than the outflow. To determine if this concept matched the field data, continuous mixing where inflow is more than the outflow was modeled. Results were compared to the collected field data to determined that continuous flow where inflow is more than the outflow does produce the desired results.

Outflow at the modeled spring (Q_{SPG}) was set to the max outflow of BMS' actual discharge (1.1 cms). This was done to simplify the model because using a changing discharge amount would add unnecessary complexity to the model. This value was used in combination with the calculated discharge from the spring to determine what the EC of the modeled spring would be (*Figure 23*).

Model Results

Mixing of the 520 µS/cm water from the Regional Aquifer Tank and 10 µS/cm rainwater from the Siphon Tank did not create the desired effect on the models EC chemograph. The EC of the modeled spring dropped too quickly when compared to the field data (*Figure 23*). The model was too simple to accurately describe the real world siphon. A pre-siphon mixing component was added to the model to decrease the rate at which the EC of the model's discharge changes.

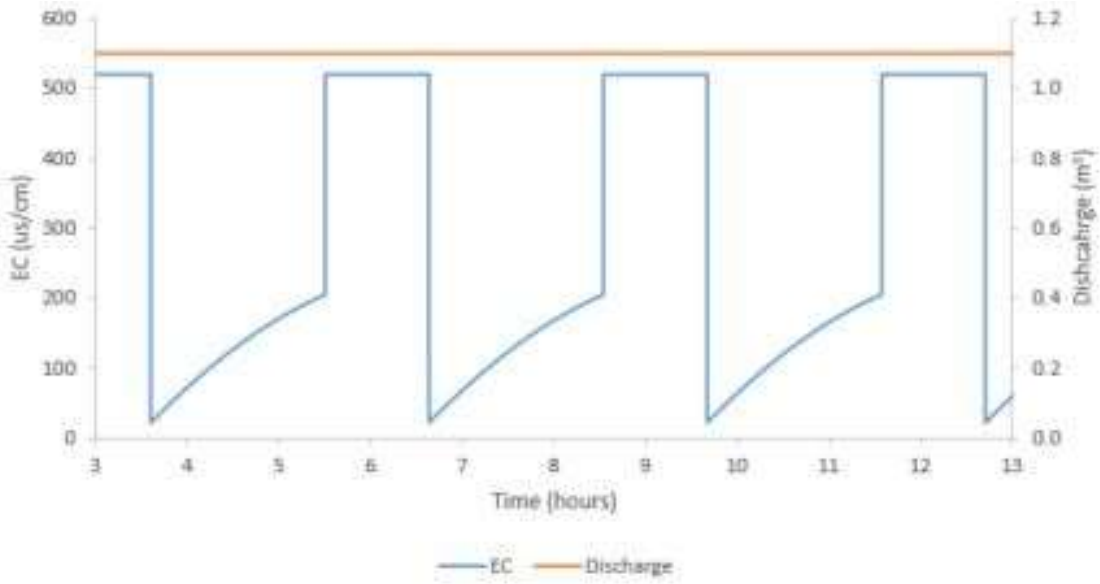

Figure 23: The effect of T-Junction mixing on EC vs the modeled discharge.

Pre-Siphon Mixing

The siphon model was integrated with a model of EC mixing in a tank to determine the EC of the siphon's discharge. The mixing model for the Siphon-Tank was created to simulate how low EC (precipitation) entering the Siphon-Tank from the surface affected the EC of the aquifer water contained in the Siphon-Tank. As low EC precipitation mixes with the equilibrium aquifer water in the tank the EC of the Siphon-Tank' water lowers.

Numerical Model

The Siphon-Tank represents a recharge feature(s) connected to secondary porosity. Surface runoff from recent precipitation events recharges the shallow aquifer and fills shallow secondary porosity.

This runoff is modeled with an EC of approximately 10 µS/cm as the EC of precipitation (Zdeb, 2018). The existing groundwater in the Siphon-Tank is modeled to have the same EC as equilibrium aquifer water (520 µS/cm). As more precipitation mixes with the existing water the EC of the water within the Siphon-Tank trends toward 10 µS/cm (*Figure 24*). The Siphon-Tank periodically drains (discussed in the following section), flushing all the water out of the tank. After the Siphon-Tank is drained, more precipitation flows into the Siphon-Tank and the water inside will only consist of precipitation with an EC of 10 µS/cm.

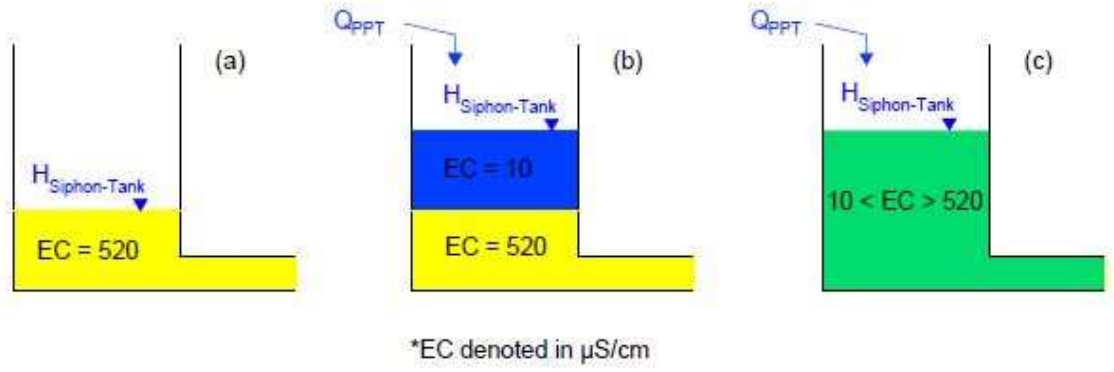

Figure 24: Pre-Siphon Mixing – (a) Siphon-Tank contains only equilibrium aquifer water with an EC of 520 µS/cm. (b) PPT with an EC of 10 µS/cm is added to the Siphon-Tank. (c) PPT mixes with equilibrium aquifer water to create water with an EC between 10 µS/cm and 520 520 µS/cm in the Siphon-Tank.

The mixing of the precipitation and equilibrium aquifer water in the Siphon-Tank was mathematically simulated using the following differential equation (Equation (13-16)) (Holzner 2008, Agarwal 2019).

$$\frac{dC}{dt} = (\text{Rate in}) - (\text{Rate out}) \tag{16}$$

$$\text{Rate in} = C_{PPT} * Q_{PPT} \tag{17}$$

$$\text{Rate out} = \frac{M(t)}{\text{Total Volume}} * Q_{S/W} \tag{18}$$

$$\frac{dC}{dt} = (C_{PPT} * Q_{PPT}) - \left(\frac{M(t)}{\text{Total Volume}} * Q_{S/W}\right) \tag{19}$$

where C(t) is the concentration of the discharge from the Siphon-Tank (includes weir flow) (µS/cm); C_{PPT} is the concentration of precipitation inflow (µS/cm); Q_{PPT} is the rate of precipitation inflow flow rate (cms); $Q_{S/W}$ is the rate of Siphon or Weir outflow (cms).

Model Calibration

The rate at which the mixing occurs in the Siphon-Tank is controlled by the amount of water present in the tank at the start of mixing and the inflow rate of precipitation. The mixing rate will increase if the inflow rate is increased and/or the existing water levels are decreased. The mixing rate will decrease if the inflow rate is decreased and/or the existing water levels are increased.

For this model, it was simulated that precipitation mixed with the Siphon-Tank half-full of equilibrium aquifer water. As precipitation is added to the existing water with an EC of 520 µS/cm, the EC of the tank lowers toward a steady-state of 10 µS/cm. With the tank half full, the mixing time could be sped up by increasing the rate at which precipitation was entering the Siphon-Tank, while the mixing time could be slowed down by decreasing the rate at which precipitation was entering the Siphon-Tank. The time it takes for the Siphon-Tank's water to reach a steady-state can also be adjusted by starting the model with more or less equilibrium aquifer water. The mixing time could be sped up by decreasing the amount of 520 µS/cm water in the Siphon-Tank, while the mixing time could be slowed by increasing the amount of 520 µS/cm water in the Siphon-Tank.

Model Results

In the field fluid EC data, the EC did not drop to 10 μS/cm for each oscillation. Additionally, the drop in EC took a longer period of time (~4.5 hours) than the rebound to base EC conditions (~ 0.5 hours). This was incorporated in the model by pre-siphon mixing of rainwater and equilibrium aquifer water. It is likely that some amount of equilibrium aquifer water remains in or flows into the siphon flowpath between each discharge event raising the EC of the siphon flowpath's discharge. Based on the field setting with two separate losing streams heading to the stream, it is unlikely a single mixing chamber would fully model the system. This interpretation explains the differences in oscillation events and the difference in time between the decrease in EC and the return to equilibrium conditions. The pre-siphon mixing model reproduces this behavior as a mechanism to generate the observed field pattern.

The mixing of existing equilibrium water and rainwater occurring in the Siphon-Tank was simulated with Equation 11. As rainwater enters the tank it mixes with the equilibrium aquifer that already exists in Siphon-Tank water decreasing the fluid EC in the tank. When head levels rise to H_2, the Siphon-Tank drains, flushing out all the water within the tank and making room for new precipitation inside. After the flushing occurs, the Siphon-Tank fills with precipitation with an EC 10 μS/cm (*Figure 25*).

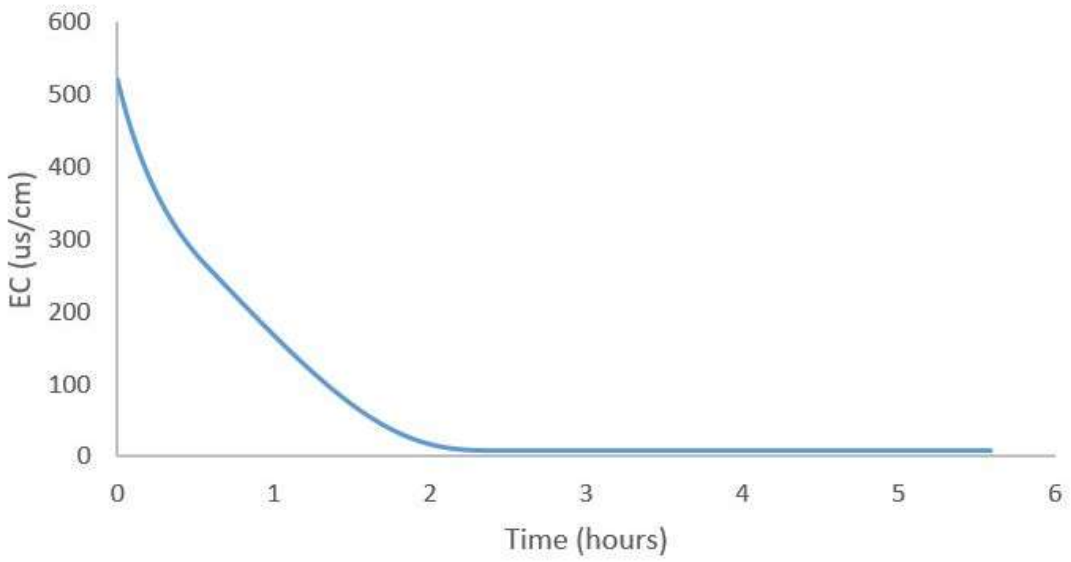

Figure 25: Siphon-Tank- Pre-Siphon Mixing simulation showing the fluid EC in the Siphon-Tank over time as rainwater is mixed with existing aquifer water in the Siphon Tank.

Combined Mixing Model

The Regional Tank Model, the Siphon Tank Model, the Pre-Siphon Mixing Model, and the T-Junction Model are combined to create a model that more accurately represents the spring. This model to calibrated to match the oscillation pattern observed in the field data. The results are then verified by comparing real-world conditions to the model's outputs.

Model Results

The Siphon, Regional Aquifer, and Pre-Siphon Mixing models are combined to create the T-junction mixing model that produces modeled fluid EC chemographs for BMS. Water from both tanks passes through the T-junction to discharge at BMS; the discharging water's fluid EC is dependent on the quantity and fluid EC of the water flowing from the Siphon-Tank (the siphon). When $Q_{PPT} > Q_{Weir} < Q_{Siphon}$ conditions occur in the Siphon-Tank, the oscillating discharge affects the EC of BMS's discharge so that it is also oscillating (*Figure 26*).

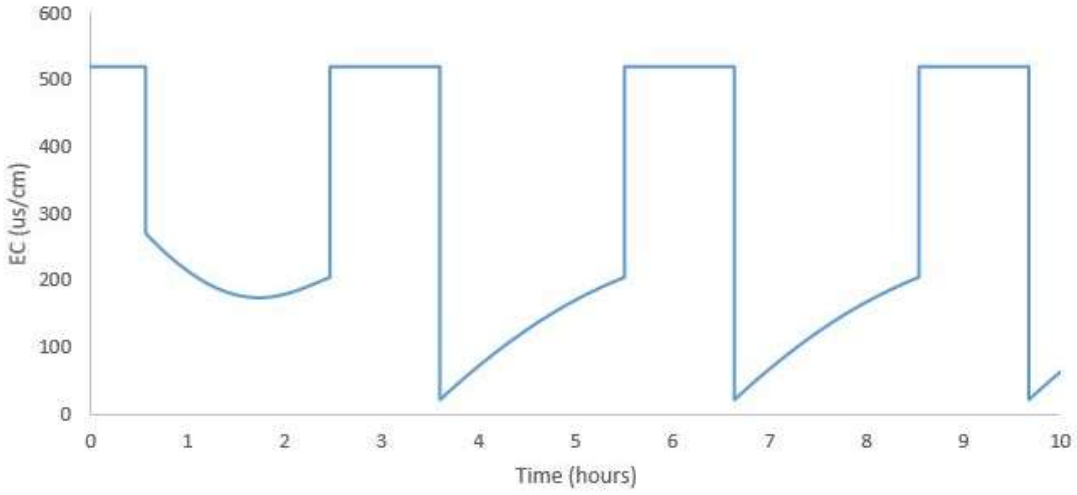

Figure 26: Modeled Electrical Conductivity of Spring Discharge with combined outputs of Pre-Siphon Mixing, Siphon Discharge, and Regional Aquifer Discharge models.

Pre-siphon mixing was only modeled one time. The mixing caused the EC of the spring's discharge not to drop completely to 10 µS/cm on the first oscillation. If equilibrium aquifer water is not added to Siphon-Tank, the tank will be flushed out and all siphon discharge will be pure rainwater (*Figure 27*).

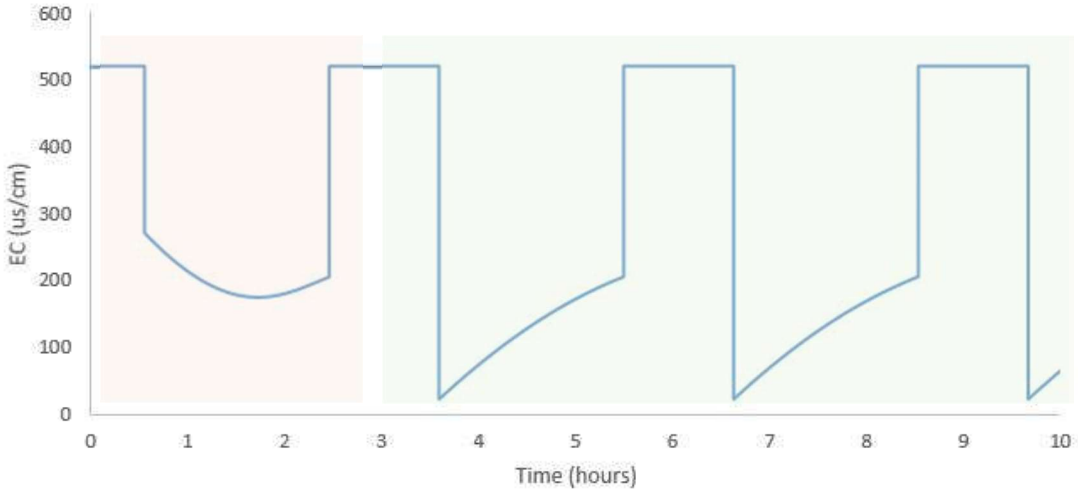

Figure 27: Tank 1 Mixing Effect on Spring – Discharge affected by pre-siphon mixing in the orange shading; Discharge not effected by pre-siphon mixing in the green shading.

As shown in the Siphon Pipe section of Results, there are three general rates at which precipitation enters the Siphon-Tank: $Q_{Weir} < Q_{PPT} > Q_{Siphon}$, $Q_{PPT} > Q_{Weir}$ and Q_{Siphon}, $Q_{PPT} < Q_{Weir}$. Each of which leads to the siphon pipe discharging differently. Because the EC of the spring is influenced by the siphon's pipe discharge, these Q_{PPT} scenarios will impact the shape of the spring EC hydrograph.

If $Q_{Weir} < Q_{PPT} > Q_{Siphon}$, the siphon will continually prime and unprimed, bringing different fluxes of water to the spring. These will cause the EC of the spring to oscillate between 520 µS/cm and 10 µS/cm (*Figure 28*).

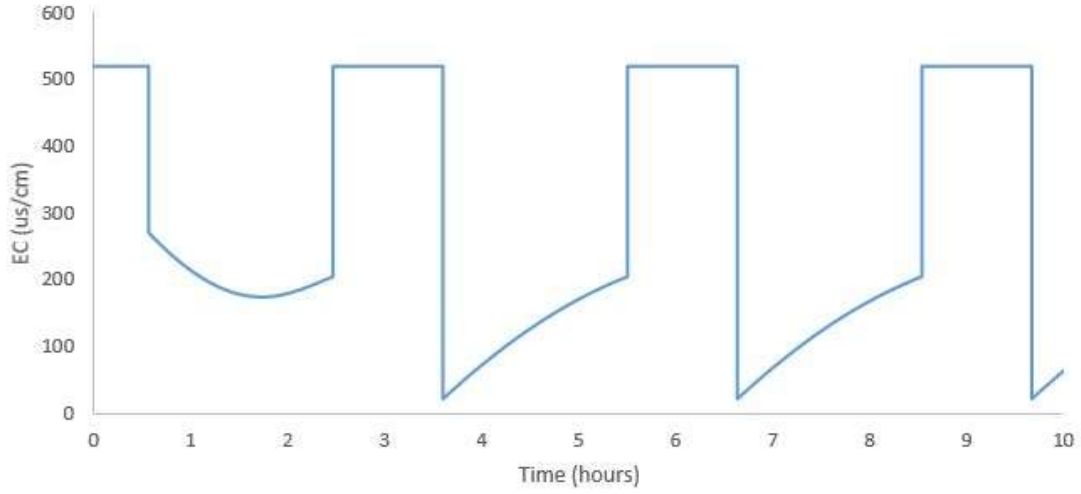

Figure 28: EC Chemograph when $Q_{Weir} < Q_{PPT} > Q_{Siphon}$

If $Q_{PPT} > Q_{Weir}$ & $Q_{Siphon\text{-}Min}$, the siphon will prime and never unprime, bringing a constant flow of water with an EC of 10 µS/cm to the spring. The constant flow will mix with the regional aquifer and cause the EC of the spring's discharge to be between 520 µS/cm and 10 µS/cm (*Figure 29*).

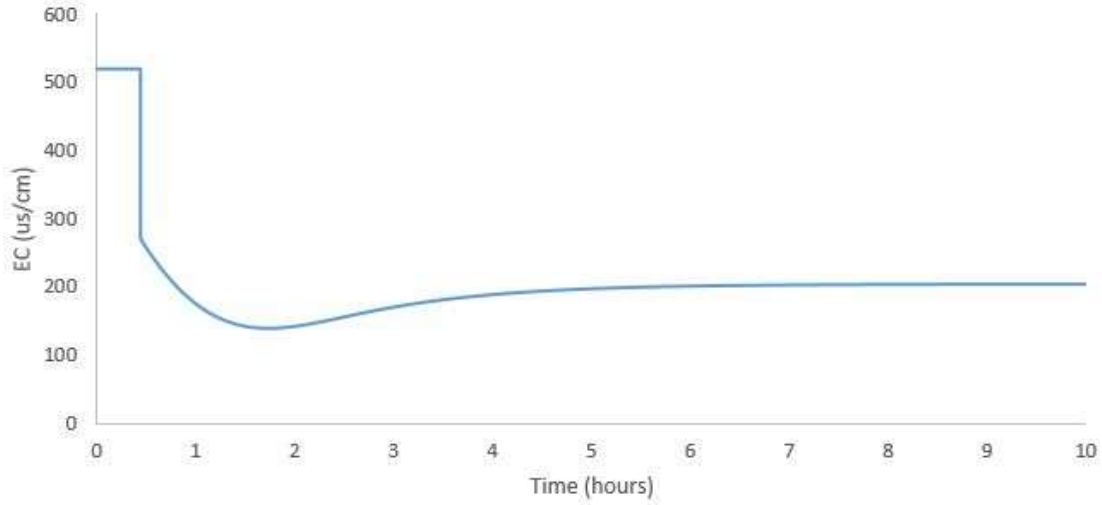

Figure 29: EC Chemograph when $Q_{PPT} > Q_{Weir}$ & $Q_{Siphon\text{-}Min}$

If $Q_{PPT} > Q_{Weir}$ & $Q_{Siphon\text{-}Max}$, the siphon will prime and never unprime, bringing a constant flow of water with an EC of 10 µS/cm to the spring. The constant flow will overwhelm the flow of the regional aquifer and cause the EC of the spring's discharge to stay at 10 µS/cm (*Figure 30*).

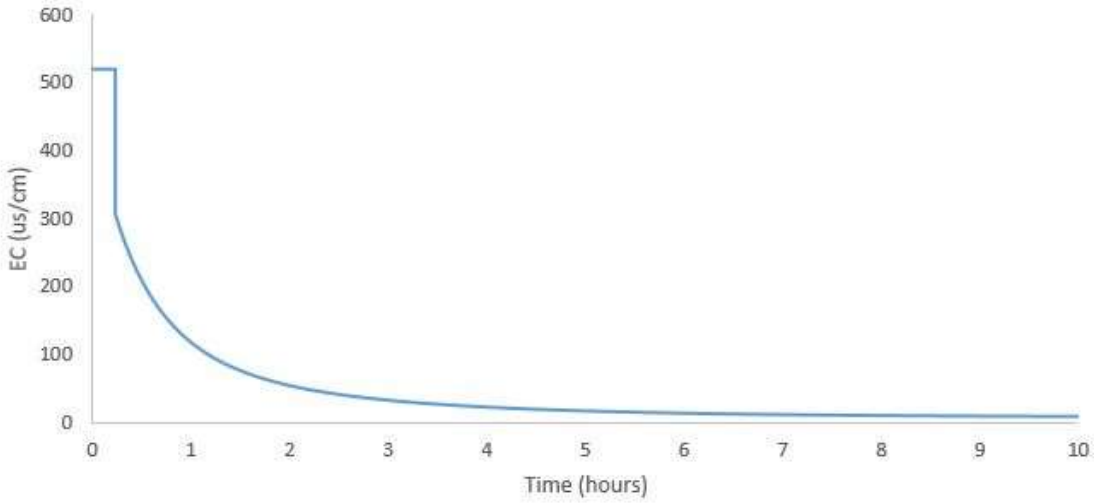

Figure 30: EC Chemograph when $Q_{PPT} > Q_{Weir}$ & $Q_{Siphon\text{-}Max}$

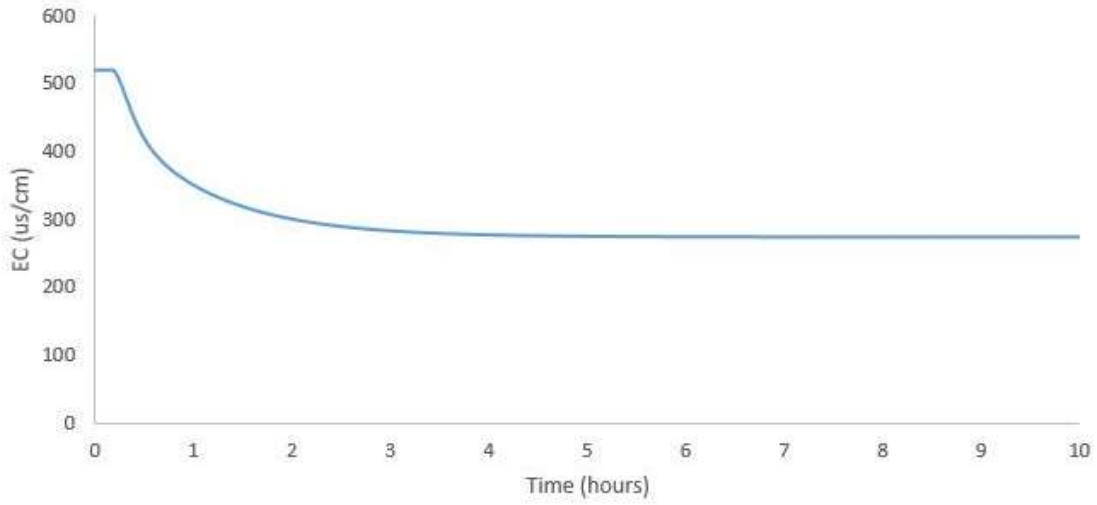

Figure 31: EC Chemograph when $Q_{PPT} < Q_{Weir}$

Model Calibration

The Siphon-Tank size was calibrated using the amount and frequency of oscillations that were observed in the field data. The field data showed that the real world siphon tank drains in approximately two hours. During the 48-hour period of interest between 5/23/15 and 5/25/15, there were 16 major oscillations observed in the field data. This information was used to determine the volume and size of the modeled Siphon-Tank. The comparison of the number of oscillations on the field data's and model's chemographs shows the differences in the model and field dataset (*Figure 32*).

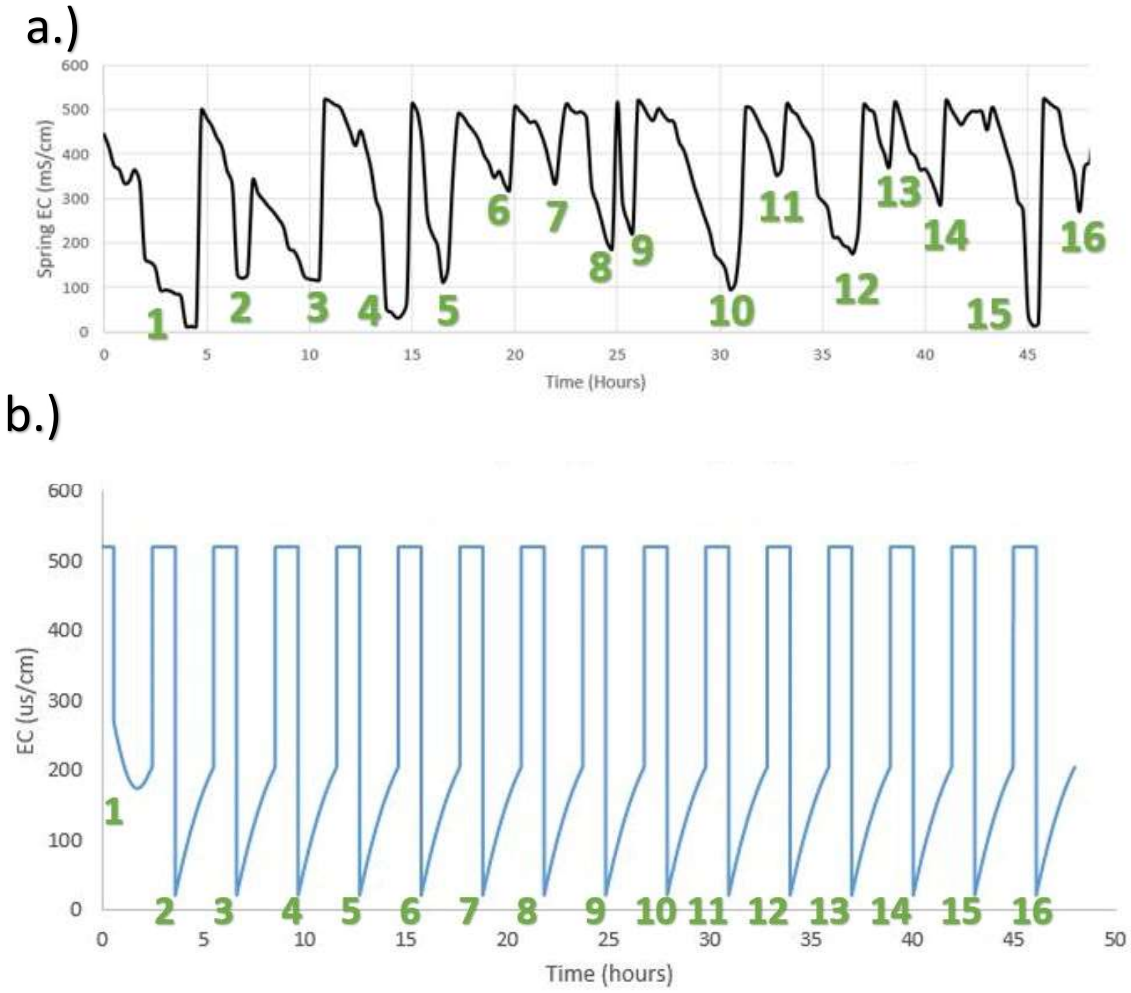

Figure 32: Comparison of BMS Field EC Data to Modeled EC Data. a.) EC chemograph constructed from collected field data showing 16 oscillations; b.) EC chemograph constructed from modeled EC data showing 16 oscillations.

Model Verification

Satellite images were searched for surface features that would provide surface waters a conveyance to the subsurface siphon within the boundaries that the model produced. Features were evaluated in the field to estimate how much flow they might be able to convey. The volume of the model tank is compared to the discharge data from the USGS gauging station at BMS.

Aerial images were searched for karst features that would act as a conveyance for precipitation to enter the subsurface within a 100 m radius. The model predicted that the siphon pipe's length was

approximately 100 m. Two intermittent streams were identified as possible points for low fluid EC precipitation to enter the subsurface (Figures 4 and 32). After the disappearing springs were observed on Google Earth a field team investigated the intermittent streams. The field team found that the streams disappeared approximately 50 m away from BMS. This 50-meter distance was used for the length of the modeled siphon pipe.

The model shows that a narrow range of parameters is required for the siphon to create oscillating EC. A small range of parameter combinations allows siphoning to repeatedly start and stop flow causing the right amount and frequency of oscillation. The siphon pipe's diameter must be the correct size for the Siphon to discharge the correct volume per time. The tank size must be the correct size or it will not drain the correct amount of times. In inflow of precipitation has to be in the correct range for it the siphon to prime and unprimed repeatedly. The model was able to produce the discharge amounts and the appropriate amount of oscillations with the values found in the $Q_{Weir} < Q_{PPT} > Q_{Siphon}$ (Table 2). The values in Table 2 were used to create *Figure 28*, *Figure 29*, *Figure 30*, & *Figure 31*:

Table 2: Siphon Model Parameters				
Parameter	$Q_{Weir} < Q_{PPT} > Q_{Siphon}$	$Q_{PPT} > Q_{Weir}$ & $Q_{Siphon\text{-}Max}$	$Q_{PPT} > Q_{Weir}$ & $Q_{Siphon\text{-}Min}$	$Q_{PPT} < Q_{Weir}$
d_s (m)	1.03	1.03	1.03	1.03
L_s (m)	50	50	50	50
H_{SPG} (m)	313	313	313	313
ξ_u	0.5	0.5	0.5	0.5
Λ_s	22.878	22.878	22.878	22.878
g (m/s^2)	9.807	9.807	9.807	9.807
H_{S3} (m)	315	315	315	315
B	0 - 1.03	0 - 1.03	0 - 1.03	0 - 1.03
H_{S2} (m)	316.9	316.9	316.9	316.9
H_{S1} (m)	318	318	318	318
Q_{PPT} (m^3/s)	0.45	1.01	0.58	.44
Tank Volume at Initial Head Conditions (m^3)	2225	2225	2225	2225

CHAPTER VII

DISCUSSION

The model was calibrated using several different variables including pipe size, tank size, and precipitation. The model outputs would change dramatically based on the inputs, but a distinct output pattern was established. The instability of this pattern tells us conditions must be within a narrow range of parameters for the siphon to operate.

The modeled fluid EC will not oscillate unless the siphon parameters are set to a small range. If there is more precipitation entering the Siphon-Tank than draining through the siphon, the Siphon-Tank head level will never drop below H_{S3} and the siphon will never turn off. If the siphon does not turn off, no oscillation will occur in the fluid EC. If there is less precipitation entering the Siphon-Tank than what flows over the weir, the siphon will never become primed and activate. If this occurs the spring fluid EC will not oscillate.

The model creates a distinct pattern of oscillating spring fluid EC, however, it does not exactly reproduce the pattern seen in the field data. The field data have a much more irregular shape than the modeled data. This irregularity is believed to be caused by an inconsistent volume of precipitation input entering the Siphon-Tank; part of the field system in a series of recharge locations along the intermittent stream beds. The model has a constant precipitation volume

entering the Siphon-Tank, which makes each fluid EC oscillation identical once the initial mixing has occurred. If the additional structure of the recharge mixing process into the Siphon-Tank were included in the model, a more realistic model output may be produced that would account for various rain size pulses and a number of recharge locations. The field data also exhibited a slower drop in fluid EC at the start of an oscillation than the modeled fluid EC. This can be explained by these same shortcomings in modeling mixing within the Siphon-Tank and is discussed further in the sections below.

To create a more accurate model relative to the field data, field values could be used for the precipitation, and stream gauging could evaluate the intermittent streams that entered the siphon system. These values could be collected from stream gauges placed on the disappearing streams that likely feed the siphon (*Figure 4* and *Figure 34*). When storm events occur, these stream gauges could measure the volume of water flowing down the streams and presumably into the siphon. The model could be fed these values to evaluate the differences between the improved model input and field EC measurements.

The plotted field data exhibited a slow drop in EC, while the model without pre-siphon mixing did not. Pre-siphon mixing corrected this by incrementally decreasing the EC of the Siphon-Tank's water to 10 μS/cm and therefore slowing the rate at which BMS's EC decreases (*Figure 33*).

(a.)

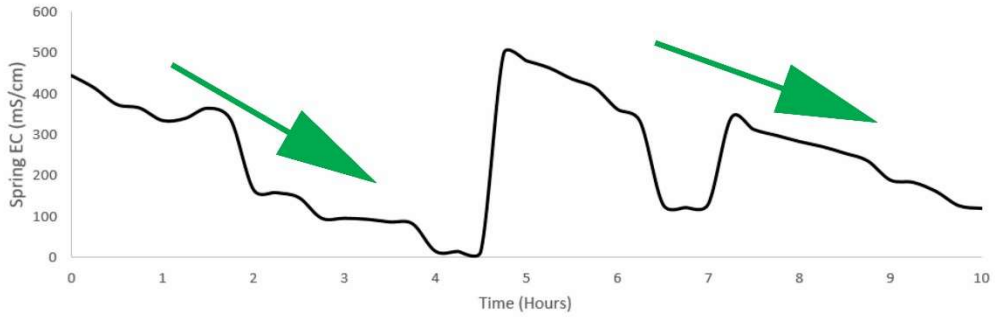

(b)

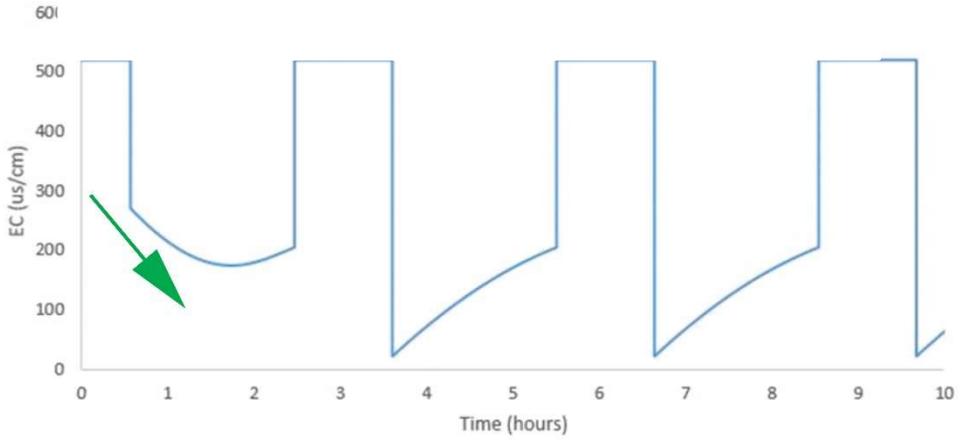

(c.)

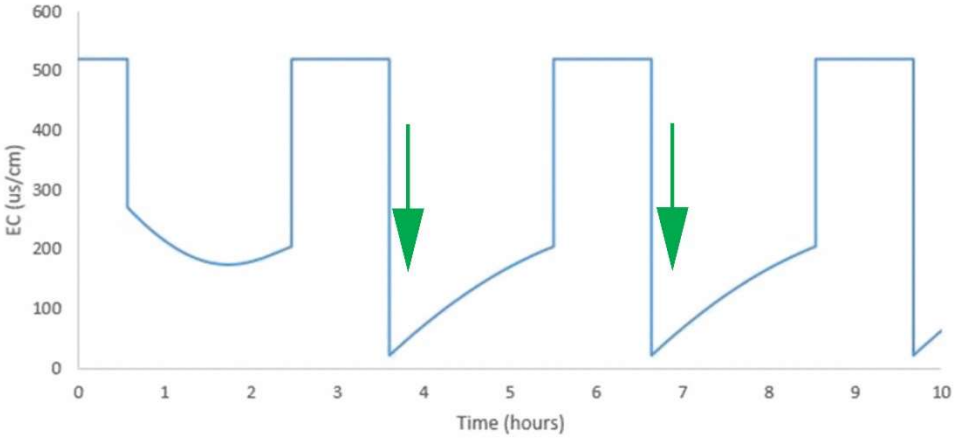

Figure 33: EC Reduction Rates – (a.) Arrows indicate the slow EC drop of BMS' field data; (b.) Arrow indicates the slow EC drop of BMS' modeled data; (c.) Arrows indicate the rapid EC drop of BMS' modeled data.

The pre-siphon mixing was assumed to be complete and total mixing. The pre-siphon mixing effect on spring EC is observed in *Figure 33*b, where there is a slower decrease in EC. In reality, the process would be more complicated. Incomplete mixing likely occurs and concentration will vary along the flowpath (García et al. 1993). However, for the purpose of this modeling experiment, this generalized explanation should be satisfactory.

The Siphon's discharge overwhelms the base flow from the regional aquifer. Flow from the regional aquifer works as an underflow spring and brings water to BMS up from depth. Flow from the siphon works as an overflow spring, which brings groundwater to the spring from higher elevations. The siphon flow can overwhelm the regional flow due to the Siphon-Tank having a higher head than the regional aquifer's outflow (BMS).

When data analysis and model creation began it was hypothesized that the Blue River may have been the source of the water that filled the Siphon-Tank during the historic rainfall events. Previous studies have shown there is a correlation in discharge amounts between the Blue River and Byrds Mill Spring. This correlation was presumed to be caused by faults that may connect the Blue River and BMS hydraulically (Halihan et al., 2009). However, based on the results of the model, the length of the siphon pipe must be located within 100 meters from BMS. Satellite imagery was checked for signs of possible karst windows within a 100-meter radius of the spring. Evidence of two intermittent disappearing streams was found (*Figure 34*).). In the field, these two streambeds merge above the spring and disappear. The model points to these streams as the most likely locations for precipitation to enter the field siphon.

The Blue River is located too far away from BMS for the model to produce the observed EC trends in the spring and provide realistic spring discharge amounts. The EAR sinkhole was also considered as a possible conveyance for rainwater to enter the spring, but the model was not able to produce the desired outputs at the distance.

The Blue River may still have a connection to BMS, but that connection most likely does not pass through the siphon, at least before converting to an equilibrium EC. Additionally, studies will have to be done to extrapolate this connection.

The West Spring Creek formation is prone to faulting in addition to karstification (Puckette, 2020; Musselman, 1994). Although the siphon structure is located in a karst aquifer the siphon may have formed due to faulting. A geophysical survey could be conducted to determine the presence of the siphon. Electrical resistivity imaging (ERI) would serve as an excellent tool to confirm the presence of the Siphon-Tank void and siphon. ERI could confirm the presence of a void below the intermittent streams and give insight into if the siphon is comprised of a fault or cave passage.

Figure 34: Disappearing Streams (Earth, 2018)

BMS is a valuable water resource to the City of Ada, efforts have already been made to protect the spring from contamination by sealing the spring in a concrete vault soon after the water supply was purchased by the city in the early 20th century (Ada, 2020; OWRB, 2007). Additional efforts should be made to protect BMS from contamination from the siphon's source water in the uplands area. The siphon should be considered to be a potential pathway for contamination to enter the spring as it directly connects the spring to a land surface and provides an obvious path for surface water to the water supply.

Actual precipitation amounts for the 0.5 km^2 surface drain basin of BMS would not be enough to trigger the extended amounts of oscillations observed in the field data (Christenson et al., 2011). The siphon's basin should be considered a potential source of contamination to BMS. This basin should be delineated and additional precautions should be made to protect the recharge area from contamination.

The model shows that local flow through the siphon can overwhelm regional aquifer flow. Water from the model Siphon-Tank and the Siphon-Tank's flow at the T-junction cuts off the Regional-Tank's flow when siphon flow becomes larger than regional flow. At this point, the EC of BMS can drop to 10 µS/cm in the model. This effect is quantitatively similar to the field data at BMS. This provides an alternative management strategy of not using spring flow when EC drops significantly.

If the flow from the siphon did not overwhelm flows from the regional aquifer, the EC of the spring would not drop to 10 µS/cm. If the water from the Siphon-Tank and Regional-Tank simply mixed, the resulting water would have an EC somewhere in between 10 µS/cm and 520 µS/cm. The combination of low EC and oscillating EC suggests that the siphon and the adjacent intermittent

streams are a more likely source of the signal than a fast flowpath through the broader regional flow system.

CHAPTER VIII

CONCLUSIONS

Byrds Mill Spring near Fittstown, Oklahoma is an underflow spring with highly stable baseflow. The spring's temperature and fluid EC are constant, except during extreme rainfall events. BMS is an important spring in that it is the largest spring by discharge in Oklahoma and a water supply to the region. Understanding the hydrogeology of events which bring untreated surface water to this spring helps us understand how to better protect spring water resources.

BMS was found to have strong fluid EC oscillations during a month of extreme precipitation events. These oscillations brought the EC from a stable value of approximately 520 µs/cm to a low of approximately 10 µs/cm. The level of fluid EC of BMS during high precipitation events indicates that during high discharge of the spring, the flow system can be composed of nearly pure rainwater, blocking the baseflow of the spring. The field data oscillations suggest that a siphon flow mechanism is overwhelming the regional flow.

An analytical tank siphon model was able to produce a distinct EC pattern that resulted from a siphon controlling a recharge path to the spring. This pattern of the frequency of the oscillation allowed for calibration of the conduit geometry of the spring. The oscillating EC chemograph data is interpreted to represent a recharge flowpath controlled by a siphon and is supported by the analytical model. The fluid EC chemograph pattern cannot be produced solely by the siphon

mechanism; there must be a base flow from the regional aquifer. Mixing at a model T-junction allows the spring to maintain a relatively constant discharge while the EC data changes significantly. Without this mixing of two flowpaths, the model could not produce the observed hydrograph and EC chemograph.

The calibrated model parameters indicate that the siphon flowpath is in close proximity to the spring (~100 meters or less). Two intermittent, disappearing streams exist upgradient of the spring within this distance. These drainages can provide a quick flow path to the spring that would be consistent with the spring flow data, and would be supported by the model as the mechanism to generate the low fluid EC signatures of the storm events. The data and model suggest the spring water quality can be protected by protecting the nearby intermittent streams from contaminant sources.

This study illustrates the value of chemograph monitoring of springs to evaluate water quality and to interpret the hydrogeology of these systems. Without the fluid EC dataset, changes in water quality in storm samples would be difficult to interpret and appropriate measures to protect the spring would be difficult to ascertain. The study illustrates that relatively small recharge features can overwhelm the water quality of a regional flow system generating an oscillatory change in water quality. Monitoring quality along with quality on a temporal basis allows an improved understanding of spring hydrogeology.

REFERENCES

Abongwa, P. T., Puckette, J. O., Atekwana, E. A., Halihan, T. (2018). "Aquifer Geology and Water Chemistry: Case of Selected Surface Water and Groundwater in Oklahoma, USA." The Shale Shaker 69(3): 126-135.

ArcMap. (2020). Esri.

Ada, City of; "Our Location, Vision & History."; Retrieved 4/20/2020; from http://www.adaok.com/About/.

Agarwal, R. P. (2019). *500 Examples and Problems of Applied Differential Equations*, Cham: Springer International Publishing: Imprint: Springer.

Atkinson, T. C. (1977). "Diffuse Flow and Conduit Flow in Limestone Terrain in the Mendip Hills, Somerset (Great Britain)." Journal of Hydrology 35(1): 93-110.

Bonacci, O. and Bojanić, D. (1991). "Rhythmic Karst Springs." Hydrological Sciences Journal 36(1): 35-47.

Brock, F. V., Crawford, K. C., Elliott, R. L., Cuperus, G. W., Stadler, S. J., Johnson, H. L., and Eilts, M. D. (1995). "The Oklahoma Mesonet: A Technical Overview." J. Atmos. Oceanic Technol. 12.

Campana, M. E. and Mahin, D. A. (1985). "Model-Derived Estimates of Groundwater Mean Ages, Recharge Rates, Effective Porosities and Storage in a Limestone Aquifer." Journal of Hydrology 76(3): 247-264.

Christenson, Scott, Hunt, A.G., and Parkhurst, D.L. (2009). Geochemical investigation of the Arbuckle-Simpson aquifer, South-central Oklahoma, 2004–06: U.S. Geological Survey Scientific Investigations Report 2009–5036, 50 p.

Christenson, Scott, Osborn, N.I., Neel, C.R., Faith, J.R., Blome, C.D., Puckette, James, and Pantea, M.P. (2011). Hydrogeology and simulation of groundwater flow in the Arbuckle-Simpson aquifer, south-central Oklahoma: U.S. Geological Survey Scientific Investigations Report 2011–5029, 104 p.

Crittenden, J. (2012). *MWH's Water Treatment: Principles and Design*, Third Edition. 3rd ed. Hoboken, N.J: John Wiley & Sons.

Earth, G. (2018). Google.

Evett, J. B. and Liu, C. (1989). *2500 Solved Problems in Fluid Mechanics and Hydraulics*. New York, McGraw-Hill.

García, A., García. L., Díaz, M. (1993). "Mixing in Unstirred Batch Fermenters." The Chemical engineering journal 51.3: B57–B61.

Halihan, T., Mouri, S., and Puckette, J. (2009). Evaluation of fracture properties of the Arbuckle-Simpson aquifer: Final report submitted to the Oklahoma Water Resources Board, Oklahoma State University School of Geology, 64 p.

Halihan, T., Wicks, C., Engeln, J. (1998). "Physical Response of a Karst Drainage Basin to Flood Pulses: Example of the Devil's Icebox Cave System (Missouri, USA)." Journal of Hydrology, v. 204, p. 24-36.

Halihan, T. and C. M. Wicks (1998). "Modeling of Storm Responses in Conduit Flow Aquifers with Reservoirs." Journal of Hydrology, v. 208, p. 82-91.

Holzner, S. (2008). *Differential Equations for Dummies*. Hoboken, NJ, Hoboken, NJ : Wiley Pub.

Johnson, J., Brown, S., and Stockman, H. (2006). "Fluid Flow and Mixing in Rough-Walled Fracture Intersections." Journal of Geophysical Research: Solid Earth 111.B12 (2006): B12206.

Kestin, S. (1978). "Viscosity of Liquid Water in the Range −8 °C to 150 °C." Journal of physical and chemical reference data 7.3: 941–948.

Lidke, D. J. and C. D. Blome (2017). "Geologic Map of the Fittstown 7.5' Quadrangle, Pontotoc and Johnston Counties, Oklahoma: U.S. Geological Survey Scientific Investigations Map 3371", U.S. Geological Survey.

McPherson, R. A., C. Fiebrich, K. C. Crawford, R. L. Elliott, J. R. Kilby, D. L. Grimsley, J. E. Martinez, J. B. Basara, B. G. Illston, D. A. Morris, K. A. Kloesel, S. J. Stadler, A. D. Melvin, A.J. Sutherland, and H. Shrivastava (2007). "Statewide Monitoring of the Mesoscale Environment: A Technical Update on the Oklahoma Mesonet." J. Atmos. Oceanic Technol. 24.

Musselman, J. L., (1994). Paleokarstic Phenomena, Depositional Environments, and Diagenesis of the Lower Ordovician West Spring Creek Formation, Arbuckle Group, in Southern Oklahoma. Oklahoma State University. The Shale Shaker, Volume 46

Oklahoma Water Resources Board (2007). "Arbuckle Simpson Hydrology Study", Arbuckle-Simpson Newsletter, Oklahoma Water Resource Board.

Park, Y. J. and Lee, K. K. (1999). "Analytical Solutions for Solute Transfer Characteristics at Continuous Fracture Junctions." Water Resources Research 35(5): 1531-1537.

Puckette, J. O. (2009). Characterization of the Arbuckle-Simpson Aquifer. Stillwater, Okla., Stillwater, Okla. : Oklahoma State University, Boone Pickens School of Geology.

Puckette, J. (2020). Personal Communication.

Rahi, K, and Halihan, T. (2009). Estimating Selected Hydraulic Parameters of the Arbuckle-Simpson Aquifer from the Analysis of Naturally-Induced Stresses. Stillwater, Okla: Boone Pickens School of Geology, Oklahoma State University.

Stevanović, Z. (2019). Karst Aquifers in the Arid World of Africa and the Middle East: Sustainability or Humanity? Karst Water Environment: Advances in Research, Management and Policy. T. Younos, M. Schreiber and K. Kosič Ficco. Cham, Springer International Publishing**:** 1-43.

Swinea, J. (2012). Thermal Controls on Springs in the Eastern Arbuckle-Simpson Aquifer System. M.S. Thesis, Oklahoma State University, Stillwater, OK

Spears, K. W. and Halihan, T. (2014). Hydrogeophysical Evaluation of Flowpaths to Byrd's Mill Spring, Oklahoma. Geological Society of America 48th South Central Sectional Meeting. Fayetteville, AR: No. 1.

Turcotte, D. L., Schubert, G. (2002). Geodynamics. 2nd ed. Cambridge; Cambridge University Press.

White, W. B. (1988). *Geomorphology and Hydrology of Karst Terrains*. New York, New York : Oxford University Press.

VITA

John Garrett Richins

Candidate for the Degree of

Master of Science

Thesis: ANALYTICAL MODELING OF CONDUCTIVITY CHEMOGRAPHS OF BYRDS MILL SPRING

Major Field: Geology

Biographical:

Education:

Completed the requirements for the Master of Science in Geology at Oklahoma State University, Stillwater, Oklahoma in December, 2020.

Completed the requirements for the Bachelor of Science in Geology at Oklahoma State University, Stillwater, Oklahoma in 2014.

Experience:

Environmental Geologist at Enercon Services in Oklahoma City, Oklahoma from July 2017 to March 2020.

Associate Professional at SCS Engineers in Yukon, Oklahoma from March 2017 to July 2017.

Environmental Scientist at Talon/LPE in Oklahoma City, Oklahoma from June 2014 to March 2017.